https://doi.org/10.5194/egusphere-2026-2751
Preprint. Discussion started: 16 June 2026

O_2:CO_2 exchange ratio and isotopic composition of atmospheric O_2 measured using soil chambers, and their application to evaluating enhanced rock weathering and the Dole–Morita effect

Shigeyuki Ishidoya[1], Takahisa Maeda[1], Hidehiko Kikuno[2], Jumpei Fukumasu[3], Shinya Iwasaki[4], Sadao Eguchi[3], Rota Wagai[5], Kei Asada[3], Taku Nishimura[5], Takuhei Yamasaki[5], Shinji Suzuki[2], Shohei Murayama[1,6], Atsushi Yamamoto[1], Asaka Hasegawa[1], Satoshi Sugawara[7], Shuji Aoki[8], and Takakiyo Nakazawa[8]

[1]National Institute of Advanced Industrial Science and Technology (AIST), Tsukuba 305-8569, Japan,
[2]Tokyo University of Agriculture, Setagaya-ku 156-8502, Japan,
[3]National Agriculture and Food Research Organization, Tsukuba 305-8517, Japan,
[4]Japan International Research Center for Agricultural Sciences, Tsukuba 305-8586, Japan,
[5]The University of Tokyo, Bunkyo-ku 113-8654, Japan,
[6]Dokkyo University, Soka, 340-0042 Japan,
[7]Miyagi University of Education, Sendai 980-0845, Japan,
[8]Tohoku University, Sendai 980-8578, Japan.

Correspondence to: Shigeyuki Ishidoya (s-ishidoya@aist.go.jp)

Abstract. Soil chamber measurements of $\delta(O_2/N_2)$, CO_2 amount fractions, and the $\delta(^{18}O)$ of O_2 in air ($\delta_{atm}(^{18}O)$) were conducted at a forest site in Takayama (TKY), Japan, and at agricultural fields in Tsukuba (TKB) and Miyakojima (MYK), Japan. The latter two fields included plots with and without crushed rock application for the evaluation of enhanced rock weathering (ERW) for carbon dioxide removal (CDR). The 7-year average O_2:CO_2 molar exchange ratios for soil–air O_2 and CO_2 fluxes were 1.10 ± 0.01 at TKY, whereas the two-year averages at the agricultural fields varied from 0.38 to 4.32. Assuming soil respiration yields an O_2:CO_2 ratio of 1.1, we partitioned measured CO_2 fluxes into soil respiration and abiotic reactions including CO_2 dissolution and dissociation processes. At TKB, the low CO_2 emissions from the basalt-applied plot were attributed to reduced soil respiration. In contrast, at MYK, both plots showed abiotic CO_2 uptake, comparable to modeled CDR rates for ERW, regardless of basalt/olivine application. These results suggest that inherent soil processes such as alkalinity-driven CO_2 absorption and leaching, rather than rock application, were responsible for the observed net CDR, questioning the impact of ERW at these sites. Our analytical approach effectively quantified CDR by accounting for both biotic and abiotic processes. The isotopic effect of soil respiration (ε_{SR}) from $\delta(O_2/N_2)$ and $\delta_{atm}(^{18}O)$ was substantially lower at

https://doi.org/10.5194/egusphere-2026-2751
Preprint. Discussion started: 16 June 2026

TKB and MYK than previously reported. Revising the plausible global average ε_{SR} to 14.6 ‰ would reduce the modeled Dole–Morita effect from 23.16 ‰ to 22.71 ‰.

1 Introduction

Simultaneous analysis of the ratio of O_2 to N_2 in the atmosphere relative to a reference O_2/N_2 ratio (i.e., $\delta(O_2/N_2)$) and the mole fractions of CO_2 in the atmosphere has been used to evaluate carbon cycles, such as uptake of CO_2 by the terrestrial biosphere and ocean (e.g., Manning and Keeling, 2006; Tohjima et al., 2019). This approach makes use of the molar oxidative ratios (OR $= -(\Delta O_2)/(\Delta CO_2)$) for terrestrial biospheric activities and fossil fuel combustion. For activities in the terrestrial biosphere, ORs of 1.05 to 1.1 are generally used based on studies of elemental abundance (Keeling, 1988; Severinghaus, 1995; Worral et al., 2023). The $-O_2$:CO_2 exchange ratios (ER $= -\Delta y(O_2)/\Delta y(CO_2)$) observed for the exchange between the atmosphere and organisms or ecosystems have also been reported by past studies (e.g., Ishidoya et al., 2013a, 2015; Battle et al., 2019; Faassen et al., 2023). It should be noted that there is a distinction between ERs and ORs; the OR indicates the stoichiometry of specific materials (Faassen et al., 2023). Faassen et al. (2023) have reported values of the ER for net turbulent O_2 and CO_2 fluxes between a forest and the overlying atmosphere (hereafter referred to as "ER_{FA}") of 0.92 ± 0.17 and 1.03 ± 0.05 for daytime and nighttime, respectively, at a boreal forest site in Hyytiälä, Finland. Ishidoya et al. (2015) have reported daily mean ER_{FA} values of 0.86 ± 0.04 at the Takayama deciduous broadleaf forest site in central Japan (36°N, 137°E, 1420 m above sea level; designated as TKY in the AsiaFlux site code database). The ER_{FA} observations of both Faassen et al. (2023) and Ishidoya et al. (2015) were based on an aerodynamic method using continuously measured $\delta(O_2/N_2)$ and CO_2 amount fractions at multiple altitudes above the forest canopy. The suggestion by Ishidoya et al. (2015) that ER_{FA} values are lower during the daytime than at night implies that ORs for net assimilation and net respiration, which are the causes of the diurnal variations, are not identical. Quantification of the ER for each assimilation or respiration process is therefore important not only to validate the average OR for terrestrial biospheric activities for the analysis of global and local CO_2 budgets (e.g., Ishidoya et al., 2020; Sugawara et al., 2021; Pickers et al., 2022), but also to advance our understanding of the O_2 and CO_2 cycles in an ecosystem.

Hilman et al. (2022) have summarized the respiration quotients (RQs) and apparent respiration quotients (ARQs) of soils and tree stems reported by past studies. The RQ and ARQ are the reciprocals of the OR and ER, respectively. As can be seen from fig. 1 of Hilman et al. (2022), the ARQs for the respiration of roots, root-free soil, and stems range from 0.27 to 1.4. These ARQs correspond to ERs of 0.71–3.7. Such variable ERs for the respiration of soil and trees could be a cause of diurnal variations of ER_{FA}. Hilman et al. (2022) have also summarized the ERs measured by soil chambers. It is well known that soil chamber measurements provide estimates of the net CO_2 flux between soil and the overlying atmosphere (hereafter referred to as "soil–air") and the ER for the soil–air O_2 and CO_2 fluxes (hereafter referred to as "ER_{SA}") (Seibt et al., 2004; Ishidoya et al., 2013a). Seibt et al. (2004) have reported an ER_{SA} of 0.94 ± 0.04 in Griffin Forest, United Kingdom on 20 July 2001. Ishidoya et al. (2013a) carried out soil chamber measurements at TKY about once per month from August 2004 to October

https://doi.org/10.5194/egusphere-2026-2751
Preprint. Discussion started: 16 June 2026

2006 and from July 2011 to October 2012; they reported an average ER_{SA} of 1.11 ± 0.01. The ER_{SA} values reported by Ishidoya et al. (2013a) are very close to the OR of 1.1 reported by Severinghaus (1995) throughout the observation period. The ERs for soil pore air measured by soil tube sampling (hereafter referred to as "ER_{soil}") summarized by Hilman et al. (2022) fall within a wide range of 0.88–4.35 (i.e., ARQs of 0.23–1.14). The ER_{SA} and ER_{soil} values should correlate closely with each other because soil–air O_2 and CO_2 fluxes are driven by gradients of O_2 and CO_2 amount fractions between the soil pore air and the overlying atmosphere.

Angert et al. (2015), who recorded ARQs by sampling with soil tubes (corresponding to the reciprocal of the ER_{soil}) that were summarized by Hilman et al. (2022), have reported that deviations of the ARQ can be attributed at least partly to inorganic processes such as effects of CO_2 dissolution in soil water. The implication is that soil–air CO_2 fluxes are driven not only by the respiration of soil biota (hereafter referred to as "soil respiration") but also by inorganic processes. Angert et al. (2015) have therefore suggested that the soil–air CO_2 flux due only to soil respiration should be estimated by dividing the measured CO_2 flux by the average soil profile ARQ. The ER_{SA} will also be useful for the separation of soil respiratory and abiotic inorganic soil–air CO_2 fluxes, and, as a further advantage, conducting soil chamber measurements is generally easier than soil tube sampling. In recent years, enhanced rock weathering (ERW) (e.g., Beerling et al., 2020, 2024) has been attracting attention as a technique for carbon dioxide removal (CDR). Weathering is accelerated in soils with high CO_2 amount fraction due to soil respiration, although the chemical weathering itself is an abiotic inorganic process. Therefore, extensive observations of ER_{SA} by soil chamber measurements to separate contributions of soil respiration and inorganic processes will facilitate the evaluation of ERW.

Soil chamber measurements will also be useful for evaluating the isotopic effect of soil–air O_2 fluxes on the $^{18}O/^{16}O$ ratio of atmospheric O_2, $\delta_{atm}(^{18}O)$. Because of various processes in the global oxygen and water cycles, the $\delta_{atm}(^{18}O)$ is about 24 ‰ higher than that of ocean water, which is by definition 0 ‰ relative to Vienna Standard Mean Ocean Water. The enrichment of $\delta_{atm}(^{18}O)$ is known as the Dole–Morita effect (Dole, 1935; Morita, 1935). Recently, Ishidoya et al. (2025) have observed diurnal, seasonal, and secular changes of $\delta_{atm}(^{18}O)$, and they have proposed some applications of the observational results, such as separation of the diurnal $\delta(O_2/N_2)$ variations into biological and fossil fuel components as well as evaluation of recent secular changes of terrestrial gross primary production and photorespiration. Isotopic effects of soil respiration (ε_{SR}) was assumed to be 18 ‰ on Bender et al. (1994) by assuming the same isotopic effect with ordinary dark respiration. Luz and Barkan (2011) revised the ε_{SR} to be 15.8 ‰ based on Angert et al. (2003), who carried out soil tube sampling and analysis by mass spectrometry of various types of vegetation. In contrast, variations of $\delta_{atm}(^{18}O)$ have never been obtained from soil chamber measurements through field experiments, except for the pioneering challenge by Seibt (2003). In this regard, we can observe $\delta_{atm}(^{18}O)$ precisely by using the same measurement system used by Ishidoya et al. (2025) to provide additional ε_{SR} data to extend the results of Angert et al. (2003).

In this study, we present $\delta(O_2/N_2)$ and CO_2 amount fractions and $\delta_{atm}(^{18}O)$ obtained from our new soil chamber measurements at TKY and in agricultural fields at Tsukuba (TKB) (36°N, 140°E) and Miyakojima (MYK) (25°N, 125°E),

https://doi.org/10.5194/egusphere-2026-2751
Preprint. Discussion started: 16 June 2026

Japan. The method of soil chamber measurements updated from Ishidoya et al. (2013a) enabled us to make precise measurements of ER_{SA} and $\delta_{atm}(^{18}O)$ that we used to evaluate in detail processes related to soil–air O_2/CO_2 exchanges and ε_{DR}. The agricultural fields at TKB and MYK were also used to evaluate ERW in the Moonshot Research and Development Program of the New Energy and Industrial Technology Development Organization (NEDO). We therefore carried out soil chamber experiments in the agricultural fields with and without rock dust spreading and evaluated the contributions of inorganic CO_2 flux, including weathering.

2 Methods

2.1 Site description

Figure 1 shows the locations of the TKY, TKB, and MYK sites. The TKY forest site is located about 15 km east of the provincial city of Takayama. The soil in the forest consists of Dystric Cambisols (Uchida et al., 2005; Lee et al., 2005). Major tree species around the site are deciduous, broad-leaved trees such as birch and oak, with a canopy height of about 15–20 m, and the ground is covered with bamboo grass. Budding and leaf shedding occur in May and October, respectively, and the ground is usually covered with snow from December to April. The annual mean temperature and precipitation are about 6.5 °C and 2100 mm, respectively. The rainy season occurs in early summer, when the site is strongly affected by the Asian monsoon. A more detailed description of the TKY site can be found in Murayama et al. (2024).

The TKB agricultural field is located at the Institute for Agro-Environmental Science, National Agriculture and Food Research Organization (NARO), in Ibaraki, Japan. The soil at the site is classified as Hydric-Silic Andosol by the World Reference Base for Soil Resources (WRB) (Wagai et al., 2018). The mean annual temperature and precipitation are 13.7 °C and 1300 mm, respectively. In June 2023, we began a field experiment under a double cropping system to evaluate the effects of enhanced rock weathering (ERW) on soil properties and crop productivity. As a part of this study, we carried out soil chamber measurements at two plots: (1) soybean (June–October) and barley (November–May) grown with crushed basalt (applied once in early June 2023 at 100 t ha^{-1}, equivalent to 10 % of the plow-layer soil mass to a depth of 15 cm) and (2) the same crops and timing but without crushed basalt. Both plots also received chemical fertilizers (30 kg N ha^{-1}, 150 kg P_2O_5 ha^{-1}, and 100 kg K_2O ha^{-1} for soybean; 70 kg N ha^{-1}, 100 kg P_2O_5 ha^{-1}, and 100 kg K_2O ha^{-1} for barley) in accordance with the regional standards for NPK fertilization of these crops. Prior to sowing, the plots were tilled twice to a depth of approximately 15 cm. We also carried out soil chamber measurements once at each of four plots characterized by (1) no crops, but addition of crushed basalt and chemical fertilizers (2) no crops and no crushed basalt, but addition of chemical fertilizers; (3) crops, no crushed basalt, and no chemical fertilizers; and (4) crops, no tilling, but addition of a mixture of cattle manure compost and chemical fertilizers. Here the crops and crushed basalt treatments were identical to the treatments in the two main plots used for soil-chamber measurements.

https://doi.org/10.5194/egusphere-2026-2751
Preprint. Discussion started: 16 June 2026

The MYK agricultural field is located at the Tokyo University of Agriculture Miyako Subtropical Farm, Okinawa, Japan (25°N, 125°E). The dominant soil type at the MYK site is an argillic, calcareous, dark-red soil classified as a Chromic Luvisol (Calcaric) by the WRB or as a Shimajiri-mahji (trivial soil name), a dark red soil covering Ryukyu limestone. The mean annual temperature and precipitation are 23.8 °C and 2076 mm, respectively. In June 2023, a field experiment with a single cropping system was established to evaluate the effects of ERW on soil properties and crop productivity. During this study, we carried out soil-chamber measurements at three plots: (1) yams grown with a single application in June 2023 of crushed basalt (176 t ha^{-1}, equivalent to 10 % of the plow-layer soil mass to a depth of 15 cm); (2) the same crop with a single application in June 2023 of crushed olivine (176 t ha^{-1}, equivalent to 10 % of the plow-layer soil mass to a depth of 15 cm); and (3) the same crop without an application of crushed basalt/olivine. All plots received cattle manure compost (150 kg N ha^{-1}, 151 kg P_2O_5 ha^{-1}, and 152 kg K_2O ha^{-1}) equal to half the regional standards for cattle manure fertilization of yams. Prior to sowing, the plots were tilled by a tractor to a depth of approximately 15 cm.

2.2 Soil chamber measurements

To measure variations of $\delta(O_2/N_2)$ and CO_2 amount fractions due to soil–air O_2 and CO_2 fluxes, we collected air samples at the TKY, TKB, and MYK sites using stainless-steel, closed chambers with a volume of about 100 L (TKY) or 55 L (TKB and MYK). Each chamber had a cover over its upper part and was connected to the ambient atmosphere through a 1/16-inch outside diameter (O.D.) stainless-steel tube to minimize the pressure imbalance between the air in the soil pores and the chamber air. Four or five air samples were taken from the chamber over a period of 30–50 min after closing the cover. The air samples were collected into 760-mL Pyrex glass flasks equipped with Viton O-ring seal glass valves at both ends, or into one-liter stainless-steel flasks equipped with metal-seal valves at both ends and with silica-coated inner walls. Because the volume of the chamber was much larger than that of the sampled air, we assumed that the influx of ambient air into the chamber during the collection of air samples had a negligible impact on the chamber air. Air was introduced into a flask from a chamber via a diaphragm pump through a 1/8-inch O.D. stainless-steel tube connected to the chamber. During the introduction of air, the inner pressure of the flask was kept at an absolute pressure of 0.2 MPa using a back-pressure valve installed at the flask outlet. The air exhausted from the back-pressure valve was introduced into the chamber through another 1/8-inch O.D. stainless-steel tube connected to the chamber. After 7–8 min had elapsed for the air to circulate in the flask, the valves of the flask were closed to maintain the absolute inner pressure at 0.2 MPa. Water vapor contained in the sample air was removed by $Mg(ClO_4)_2$ that had been inserted into the air-flow line. The soil chamber measurements were carried out 23 times at TKY during the period February 2019 to August 2025, 24 times at TKB during the period November 2024 to October 2025, and 14 times at MYK during the period July 2023 to January 2026.

The samples of air collected in the flasks were sent to the National Institute of Advanced Industrial Science and Technology (AIST) to measure the $\delta(O_2/N_2)$, CO_2 amount fraction, and $\delta_{atm}(^{18}O)$ using a mass spectrometer (Thermo Scientific Delta V). The sample air was supplied from the flask at a flow rate of about 4 mL min^{-1} through a cold trap (about −50 °C), and a minuscule amount of it was introduced into the ion source (or waste line) of the mass spectrometer through a fused-silica

https://doi.org/10.5194/egusphere-2026-2751
Preprint. Discussion started: 16 June 2026

capillary (Ishidoya and Murayama, 2014). The $\delta(O_2/N_2)$ and $\delta_{atm}(^{18}O)$ are reported in per meg (one per meg is equal to 1×10^{-6}) as follows:

$$\delta(O_2/N_2) = \frac{R_{sample}(^{16}O^{16}O/^{14}N^{14}N) - R_{standard}(^{16}O^{16}O/^{14}N^{14}N)}{R_{standard}(^{16}O^{16}O/^{14}N^{14}N)}, \quad (1)$$

$$\delta_{atm}(^{18}O) = \frac{R_{sample}(^{18}O^{16}O/^{16}O^{16}O) - R_{standard}(^{18}O^{16}O/^{16}O^{16}O)}{R_{standard}(^{18}O^{16}O/^{16}O^{16}O)}. \quad (2)$$

Here, the subscript "sample" and "standard" indicate the sample air and the standard gas, respectively. Because O_2 constitutes 20.93 % to 20.94 % of air by volume (Tohjima et al., 2005; Aoki et al., 2019), 4.8 per meg of $\delta(O_2/N_2)$ is equivalent to about 1 μmol mol^{-1}. In this study, we used a mass spectrometer to determine the $\delta(O_2/N_2)$ and $\delta_{atm}(^{18}O)$ of each air sample against our primary standard air in a 48-L, high-pressure aluminum cylinder (cylinder no. CRC00045). The $\delta(Ar/N_2)$, $\delta_{atm}(^{15}N)$, and $\delta_{atm}(^{40}Ar)$ were measured simultaneously using the mass spectrometer against the primary standard:

$$\delta(^{40}Ar/N_2) = \frac{R_{sample}(^{40}Ar/^{14}N^{14}N) - R_{standard}(^{40}Ar/^{14}N^{14}N)}{R_{standard}(^{40}Ar/^{14}N^{14}N)}, \quad (3)$$

$$\delta_{atm}(^{15}N) = \frac{R_{sample}(^{15}N^{14}N/^{14}N^{14}N) - R_{standard}(^{15}N^{14}N/^{14}N^{14}N)}{R_{standard}(^{15}N^{14}N/^{14}N^{14}N)}, \quad (4)$$

$$\delta_{atm}(^{40}Ar) = \frac{R_{sample}(^{40}Ar/^{36}Ar) - R_{standard}(^{40}Ar/^{36}Ar)}{R_{standard}(^{40}Ar/^{36}Ar)}. \quad (5)$$

The reproducibility of $\delta(O_2/N_2)$, $\delta(Ar/N_2)$, $\delta_{atm}(^{18}O)$, $\delta_{atm}(^{15}N)$, $\delta_{atm}(^{40}Ar)$, and the CO_2 amount fraction for the air samples filled in the flasks were about ±5, ±8, ±3, ±1.5, ±13 per meg, and ±0.3 ppm (±1σ), respectively. The CO_2 amount fractions were determined against the Tohoku University (TU)-10 scale, which is based on gravimetrically prepared CO_2 standard air (e.g., Nakazawa et al., 1991; Sugawara et a., 2018).

Ishidoya et al. (2014, 2022) have reported measurements of the same variables for the air samples collected onboard an aircraft. From the relationships between $\delta(Ar/N_2)$, $\delta_{atm}(^{18}O)$, and $\delta_{atm}(^{40}Ar)$ with $\delta_{atm}(^{15}N)$, they found that the measured values of $\delta(O_2/N_2)$ were contaminated by significant, artificial, thermally diffusive fractionation of O_2 and N_2 during the process of collecting air samples. They corrected the fractionation effect superimposed on the $\delta(O_2/N_2)$ by using the simultaneously measured $\delta(Ar/N_2)$, variations of which are very small in the troposphere. We therefore examined the relationships between $\delta(Ar/N_2)$ and $\delta_{atm}(^{40}Ar)$ with $\delta_{atm}(^{15}N)$ for the air samples obtained from the soil chamber measurements. Figure 2 shows the measured relationships for all the air samples at TKY, TKB, and MYK. The relationships were generally close to that expected for thermally diffusive fractionation, although there were some exceptions. We decided to correct the observed $\delta(O_2/N_2)$ and $\delta_{atm}(^{18}O)$ for thermally diffusive fractionation following the method of Ishidoya et al. (2014, 2022). Specifically, we subtracted

https://doi.org/10.5194/egusphere-2026-2751
Preprint. Discussion started: 16 June 2026

(4.57/16.2) × $\delta(Ar/N_2)$ and (1.55/16.2) × $\delta(Ar/N_2)$ from the measured $\delta(O_2/N_2)$ and $\delta_{atm}(^{18}O)$, respectively. These coefficients (4.57/16.2 and 1.55/16.2) are, respectively, the $\delta(O_2/N_2)/\delta(Ar/N_2)$ and $\delta_{atm}(^{18}O)/\delta(Ar/N_2)$ ratios determined via laboratory experiments (Ishidoya et al., 2013b).

The uncertainty of measured ERs has been calculated to be no more than 3 % by Ishidoya et al. (2020) based on a comparison of CO_2 amount fractions observed by AIST and the National Institute for Environmental Studies (NIES) in the Yoyogi district (36°N, 140°E) of Tokyo. The uncertainty of measured ER that arises from the span uncertainty of $\delta(O_2/N_2)$ is very small (0.2 %) and has been determined using gravimetrically prepared standard gases developed by Aoki et al. (2019). In this study, we also used ER_{SA} values observed at the TKY site during August 2004 to August 2005 reported by Ishidoya et al. (2013a). They carried out soil chamber measurements, but the procedures for collecting air and measurement methods differed from those in the present study; they collected air samples without stabilization of the inner pressure of the flasks and did not correct for the superposition of thermally diffusive fractionation on $\delta(O_2/N_2)$.

2.3 Soil pore air and soil water content measurements

To measure vertical profiles of $\delta(O_2/N_2)$ and CO_2 amount fractions in soil pore air at the TKY site, we collected air samples through a stainless-steel air-sampling tube (O.D., 6.35 mm; inside diameter, 2.09 mm) buried in the ground. There were 20 ventilation halls with a diameter of 2 mm at the tip of the tube. Air samples taken from the ventilation halls of the tubes were used to fill 250-mL Pyrex flasks equipped with Viton O-ring seal glass valves at atmospheric pressure. The sampling depths were 10, 20, 35, 50, and 70 cm. At each depth, four air-sampling tubes connected by stainless-steel tubing (O.D. 3.18 mm) were buried. Water vapor contained in the sample air was removed by using $Mg(ClO_4)_2$. Collections of soil pore air were carried out 16 times during the period August 2004 to August 2005. The $\delta(O_2/N_2)$ and CO_2 amount fractions were measured at TU by using a mass spectrometer (Finnigan MAT-252) (Ishidoya et al., 2003) and a gas chromatograph equipped with a flame ionization detector (GC-9A, Shimadzu) (e.g., Kawamura et al., 2003; Kato et al., 2004), respectively. The reproducibility of $\delta(O_2/N_2)$ was estimated to be ±5.3 per meg (Ishidoya et al., 2003), and our intercomparison of $\delta(O_2/N_2)$, which was conducted by using gravimetrically prepared standard gases (Aoki et al., 2021), revealed that the span sensitivity of the $\delta(O_2/N_2)$ measured at TU agreed well with that at AIST. The uncertainty of the CO_2 amount fraction measured by the gas chromatograph was estimated to be about ±1 %. Soil water contents (SWCs) at TKY were measured with water content reflectometers (CS615 and CS616, Campbell Scientific) at depths of 15 and 40 cm; 30-min average values were recorded on a data logger (CR10X, Campbell Scientific). Relationships between the SWC and soil–air CO_2 flux at TKY have been discussed in previous studies (e.g., Kishimoto-Mo et al., 2015).

At TKB, CO_2 sensors (GMP-251, Vaisala), O_2 sensors (SO-210, Apogee Instrument), and temperature and moisture sensors (TEROS-12, Meter) were buried in the two main plots for soil chamber measurements (see Sect. 2.1) at depths of 10, 30, and 65 cm. There was a duplicate of only the TEROS-12 sensor at each depth. The CO_2 and O_2 amount fractions and SWC were measured by the sensors at 30-min intervals, and the measured values were recorded on a data logger (CR1000, Campbell

https://doi.org/10.5194/egusphere-2026-2751
Preprint. Discussion started: 16 June 2026

Scientific). The SWCs were also measured at MYK with an SWC sensor (10HS, METER) at depths of 5 and 15 cm. Measurements were taken at one-hour intervals and recorded by a data logger (ZL6 Basic, METER).

2.4 Separation of soil–air CO_2 flux into soil respiration and abiotic inorganic processes

We decomposed the CO_2 fluxes obtained from soil chamber measurements at TKY, TKB, and MYK into contributions from soil respiration and abiotic inorganic processes as follows:

$$F_{CO2\_R} = (-1.1)^{-1} F_{O2} \quad (6),$$

$$F_{CO2\_I} = F_{CO2} - F_{CO2_R}, \quad (7).$$

where F_{CO2} and F_{O2} are the observed soil–air CO_2 and O_2 fluxes, respectively, and F_{CO2_R} and F_{CO2_I} are the respective contributions of soil respiration and inorganic processes to F_{CO2}. We assumed that the ER for F_{CO2} and F_{O2} due only to soil respiration was 1.1 (Severinghaus, 1995) and that F_{O2} was driven only by soil respiration. We consider these assumptions to be generally valid because the ER_{SA} values at TKY were close to 1.1 throughout the observation period, and their slight deviations from 1.1 could be explained in the context of the effect of CO_2 dissolution, as discussed in Sect. 3.2 below. A caveat to this explanation is that some minor processes (e.g., Fe redox reactions) may be non-negligible under certain conditions (Angert et al., 2015), and an effect of those processes could be an ER for soil respiration different from 1.1. An example of an alternative approach is the estimation of biotic and abiotic soil–air CO_2 fluxes separately in saline and alkaline soils in China by Wang et al. (2020). They compared the soil–air CO_2 fluxes in natural soil and sterilized soil. They observed soil-to-air and air-to-soil abiotic CO_2 fluxes during the daytime and nighttime, respectively, and suggested that the effect of CO_2 dissolution was the most likely mechanism responsible for the abiotic CO_2 fluxes. The fact that the method to separate F_{CO2_R} and F_{CO2_I} used in the present study does not require sterilization of soil is an advantage over the method used by Wang et al. (2020) because we could perform the experiments without influencing the soil environment. The F_{CO2}, F_{CO2_R}, and F_{CO2_I} at TKY, TKB, and MYK will be presented in Sect. 3.3. Similar separation of soil respiration and inorganic processes but for vertical profiles of CO_2 amount fractions in soil pore air at TKY will also be presented in Sect. 3.2.

2.5 Rayleigh distillation equation to estimate ε_{SR} and diffusion–respiration model

We used the $\delta_{atm}(^{18}O)$ and $\delta(O_2/N_2)$ data obtained from the soil chamber measurements at TKY, TKB, and MYK and the Rayleigh distillation equation (Angert and Luz, 2001; Kroopnick and Craig, 1976) to estimate ε_{SR} as follows:

$$\varepsilon_{SR} = \frac{lnR/R_0}{-lnf} \quad (8)$$

https://doi.org/10.5194/egusphere-2026-2751
Preprint. Discussion started: 16 June 2026

Here, R is the $R_{sample}(^{18}O^{16}O/^{16}O^{16}O)$ of the O_2 in chamber air at the time of sampling, and R_0 is the initial ratio. We assumed that R_0 was equal to $R_{standard}(^{18}O^{16}O/^{16}O^{16}O)$ in Eq. (2). The variable f is the fraction of O_2 that remains and is calculated from the observed $\delta(O_2/N_2)$ by assuming an initial $^{16}O^{16}O/^{14}N^{14}N$ value of 0.26808 (Aoki et al., 2019). The ε_{SR} was equated to the slope of the least-squares regression line fitted to the scatter plot of $ln\, R/R_0$ and $-lnf$. The estimated ε_{SR} at TKY, TKB, and MYK will be presented in Sect. 3.4. We also used the diffusion–respiration model of Farquhar et al. (1982) that was adopted by Angert et al. (2001, 2003) and Angert and Luz (2001) for an interpretation of the estimated ε_{SR}. The equation of the model is:

$$D_{\mathrm{total}} = D_{\mathrm{d}} + (D_{\mathrm{r}} - D_{\mathrm{d}})\, C_{\mathrm{i}}/C_{\mathrm{a}} \quad (9)$$

Here D_{total}, D_d, and D_r are the overall discrimination, discrimination associated with diffusion, and respiratory discrimination, respectively. C_i and C_a are the internal and ambient O_2 amount fractions, respectively, of the site of oxygen consumption. For example, C_i is the O_2 amount fraction in root tissues, and C_a is that in soil pore air. Angert and Luz (2001) adopted a D_d of 0 ‰ because lateral diffusion within roots is thought to occur in the liquid phase, and discrimination in liquids is usually small (Armstrong et al., 1994; Farquhar and Lloyd, 1993). Angert and Luz (2001) adopted a D_r value of 18 ‰ based on measurements of isolated plant organs by Guy et al. (1989, 1993). The ε_{SR} reported in this study corresponds to D_{total} in Eq. (9).

3 Results and Discussion

3.1 $\delta(O_2/N_2)$, CO_2 amount fractions, and $\delta_{atm}(^{18}O)$ at TKY, TKB, and MYK observed by soil chamber measurements

Figure 3a shows the relationships between the $\delta(O_2/N_2)$ and CO_2 amount fractions obtained from soil chamber measurements made 23 times at TKY. The data have been color-coded by season. For all measurements, the $\delta(O_2/N_2)$ and CO_2 amount fractions decreased and increased with time, respectively, after the chamber closed. The ER_{SA} value for each observation was equated to the slope of the least-squares regression line fitted to the data. The average ER_{SA} values were 1.01 ± 0.06, 1.11 ± 0.08, 1.10 ± 0.04, and 1.05 ± 0.03 in winter, spring, summer, and autumn, respectively. We defined the time intervals of December to March (snow-covered), April and May, June to August, and September to November as winter, spring, summer, and autumn, respectively, based on the weather at TKY. The average ER_{SA} values agreed well with the OR (oxidative ratio) of 1.05–1.1 that is generally used for terrestrial biospheric activities in atmospheric $\delta(O_2/N_2)$ studies (Keeling, 1988; Severinghaus, 1995) throughout the year. Figure 3b shows the relationships between $\delta_{atm}(^{18}O)$ and $\delta(O_2/N_2)$ obtained from the soil chamber measurements at TKY. The increase of $\delta_{atm}(^{18}O)$ with decreasing $\delta(O_2/N_2)$ suggested that $^{16}O^{16}O$ was consumed preferentially to $^{18}O^{16}O$ by soil respiration during the chamber measurements. The average $\delta_{atm}(^{18}O)(\delta(O_2/N_2))^{-1}$ ratios, except

https://doi.org/10.5194/egusphere-2026-2751
Preprint. Discussion started: 16 June 2026

for those with correlation coefficients lower than 0.5, were −0.014 ± 0.004, −0.015 ± 0.003, and −0.016 ± 0.002 in spring, summer, and autumn, respectively.

Figure 4a shows the relationships between the $\delta(O_2/N_2)$ and CO_2 amount fractions obtained from 24 soil chamber measurements at TKB. The data have been color-coded for each plot. The $\delta(O_2/N_2)$ and CO_2 amount fractions decreased and increased, respectively, with time in a manner similar to the soil chamber measurements at TKY. However, the variations of the ER_{SA} were much larger than those at TKY. Specifically, the minimum and maximum ER_{SA} at TKB were 0.38 and 4.32, respectively, whereas those at TKY were 0.93 and 1.20. Because substantial variations of the ER_{SA} at TKB were apparent in the plots where crushed basalt both had and had not been spread (red/black markers in Fig. 4a), the variations were not attributed to an effect of ERW. Variations of the ER were also apparent in the plots with/without planting and chemical fertilizer. The implication is that the variations of the ER_{SA} were caused by factors other than weathering, planting, and fertilizer. Figure 4b shows the relationships between the $\delta_{atm}(^{18}O)$ and $\delta(O_2/N_2)$ obtained from the soil chamber measurements at TKB. Although the $\delta_{atm}(^{18}O)$ generally increased with decreasing $\delta(O_2/N_2)$, the changes of $\delta_{atm}(^{18}O)$ were smaller than those observed at TKY.

Figure 5a shows the relationships between the $\delta(O_2/N_2)$ and CO_2 amount fractions obtained from 14 soil chamber measurements at MYK. The $\delta(O_2/N_2)$ and CO_2 amount fractions decreased and increased, respectively, with time for all the chamber measurements. The ER values, which ranged between 0.82 and 3.35, were larger than those at TKY. Substantial variations of the ER were found for the fields both with and without application of crushed basalt or olivine. The implication is that the variations were not due to ERW. Figure 5b shows the relationship between $\delta_{atm}(^{18}O)$ and $\delta(O_2/N_2)$ at MYK. Although the $\delta_{atm}(^{18}O)$ and $\delta(O_2/N_2)$ were negatively correlated, the changes of $\delta_{atm}(^{18}O)$ were smaller than those observed at TKY. Both the substantial variations of ER_{SA} and the suppressed $\delta_{atm}(^{18}O)(\delta(O_2/N_2))^{-1}$ ratios found at TBK and MYK may therefore be characteristics of agricultural fields.

Figure 6 summarizes the relationships between $\delta(O_2/N_2)$ and the CO_2 amount fractions at TKY, MYK, and TKB. The average ER_{SA} throughout the study at TKY of 1.101 ± 0.006 agreed well with the ER_{SA} of 1.107 ± 0.010 obtained from soil chamber measurements previously reported at TKY by Ishidoya et al. (2013a) from August 2004 to October 2006 and from July 2011 to October 2012. The implication is that the range of the $\delta(O_2/N_2)$ values and CO_2 amount fractions measured at AIST were consistent with those measured at Tohoku University by Ishidoya et al. (2013a) if the soil environment affecting ER_{SA} has not changed significantly since 2004. However, it is difficult to determine averages of ER_{SA} at TKB and MYK because of the large variations described above. In Sect. 3.2, we discuss possible causes of changes of ER_{SA}. The isotopic effects of soil respiration, ε_{SR}, estimated from the $\delta_{atm}(^{18}O)$ and $\delta(O_2/N_2)$ measured at TKY, TKB, and MYK will be discussed in Sect. 3.4.

https://doi.org/10.5194/egusphere-2026-2751
Preprint. Discussion started: 16 June 2026

3.2 Relationships of the observed ER_{SA} with soil water content and amount fractions of O_2 and CO_2 in soil pore air

Figure 7a shows the seasonal variations of the ER_{SA} at the TKY site. As described in Sect. 3.1, temporal variations of ER_{SA} were much smaller at the TKY site than at the TKB and MYK sites. Nevertheless, the ER_{SA} values at TKY were slightly higher in summer than in winter, and the seasonal maximum occurred in June. The SWCs at a depth of 15 cm are also plotted in Fig. 7a, and Fig. 7b shows the relationship between the ER_{SA} and SWC. Because the SWC also underwent seasonal variations with a maximum in summer, there was a significant positive correlation between the ER_{SA} and SWC. The fact that the correlations were positive even when the SWCs were averaged for 30 min, one day, or one week suggested that the correlation was robust.

To examine the cause(s) of the observed seasonal variations of the ER_{SA}, we compared the ER_{soil} (defined by Eq. 10 below) at TKY with the ER_{SA} and SWC. Figure 8 shows vertical profiles of the ΔO_2 and CO_2 amount fractions in soil pore air at TKY for the period from 25 August 2004 to 24 August 2005. The Δ symbols denote the deviations of the O_2 amount fractions from the atmospheric value. The ΔO_2 values were converted from the $\Delta\delta(O_2/N_2)$ data by multiplying by 0.2094 μmol mol^{-1} (per meg) $^{-1}$. The ΔO_2 and CO_2 amount fractions decreased and increased, respectively, with increasing depth, and the variations were larger in summer than in winter. If we assume the average atmospheric O_2, N_2, Ar, and CO_2 amount fractions to be 20.940 %, 78.088 %, 0.934 %, and 0.038 %, respectively, during 2004–2005 and ignore other minor atmospheric constituents, the average summertime O_2 amount fractions are calculated to be 20.4 % ± 0.4 %, 20.3 % ± 0.6 %, 20.0 % ± 0.5 %, 19.7 % ± 0.7 %, and 19.6 % ± 0.5 % at depths of 10, 20, 35, 50, and 70 cm, respectively. These values are substantially higher than those in the agricultural fields at TKB discussed below. It is apparent from Fig. 8 that changes of the ΔO_2 amount fractions were generally larger than those of CO_2. This difference cannot be attributed to the larger molecular diffusivity of O_2 compared to CO_2 in soil pore air, because that difference would make the vertical gradient of CO_2 amount fractions larger than that of ΔO_2.

We defined ER_{soil} at the TKY site as follows:

$$ER_{soil} = (0.76)^{-1}\Delta y(O_2)\Delta y(CO_2)^{-1} \quad (10),$$

Here, *y* stands for the dry amount fraction of gas, as recommended by the International Union of Pure and Applied Chemistry (IUPAC) Green Book (Cohen et al., 2007). The decimal 0.76 is the $CO_2(O_2)^{-1}$ ratio of molecular diffusivity in air at standard temperature and pressure (Angert et al., 2015; Massman, 1998), and $\Delta y(O_2)$ and $\Delta y(CO_2)$ are the ΔO_2 and changes in CO_2 amount fractions, respectively, for each vertical profile in Fig. 8. Figure 9a shows the temporal variations of the ER_{soil} and ER_{SA} observed at TKY in 2004–2005, except for the ER_{SA} during the snow-covered period. The SWC values at a depth of 15 cm at TKY are also shown in Fig. 9a. The ER_{soil} values were notably high during summer, and the SWC increased simultaneously. Figure 9b shows the relationships of ER_{soil} and ER_{SA} with SWC in July and August of 2004 or 2005. Both the summertime ER_{soil} and ER_{SA} increased with increasing SWC, and the slope of the ER_{soil} versus SWC least-squares regression line fitted to the data was about 10 times that of the ER_{SA} versus SWC regression. The implication is that variations of ER_{soil}

https://doi.org/10.5194/egusphere-2026-2751
Preprint. Discussion started: 16 June 2026

at least partly drove the seasonal variations of ER_{SA} in Fig. 7a. Moreover, the positive correlations of ER_{soil} and ER_{SA} with SWC suggest that CO_2 dissolution in soil water and dissociation to produce bicarbonate ions should be taken into account because this process lowers the CO_2 amount fractions in soil pore air. In this regard, there are some inorganic processes in soil pore air that change the CO_2 amount fractions in the absence of any oxidation reactions. These processes include dissolution of CO_2, weathering processes of clay minerals and parent materials that constitute the soil solid phase. The CO_2 dissolution and dissociation processes can be written as follows:

$$CO_2(gas) \leftrightarrow CO_2(aqua) + H_2O \leftrightarrow H_2CO_3 \leftrightarrow HCO_3^- + H^+ \leftrightarrow CO_3^{2-} + 2H^+ \quad (11).$$

As an example of the weathering, the weathering of calcium carbonate can be written as follows:

$$CaCO_3 + CO_2 + H_2O \rightarrow Ca^{2+} + 2HCO_3^- \rightarrow CaCO_3 + CO_2 + H_2O \quad (12).$$

As another example, the weathering of mafic rock is written as follows (here, olivine is shown as an example):

$$Mg_2SiO_4 + 4CO_2 + 4H_2O \rightarrow 2Mg^{2+} + 4HCO_3^- + H_4SiO_4 \rightarrow 2MgCO_3 + SiO_2 + 2CO_2 + 2H_2O \quad (13).$$

Equations (11) and (12) indicate that the effects of CO_2 dissolution and weathering of calcium carbonate are not net sinks of atmospheric CO_2, but they can remove CO_2 from the atmosphere during the period when the removed CO_2 exists as HCO_3^- and CO_3^{2-} in water. However, weathering of olivine is a net sink for 50 % of the removed CO_2 from the atmosphere. In general, the processes that weather mafic rock are very slow, and the effect of CO_2 dissolution is considered to be the main cause of the inorganic processes that affect soil–air CO_2 fluxes (e.g., Wang et al., 2020).

The above-mentioned inorganic processes do not affect the soil–air O_2 flux. The implication is that the simultaneous analysis of O_2 and CO_2 amount fractions can enable us to separate changes of CO_2 amount fractions due to biotic soil respiration from those due to abiotic inorganic processes. Because the OR for soil respiration needs to be specified for this purpose, we adopted the OR of 1.1 from Severinghaus (1995). We applied this separation method to the data in Fig. 8. First, changes of CO_2 amount fractions due to soil respiration were equated to $-\Delta y(O_2)(0.76)^{-1}(1.1)^{-1}$. Changes of CO_2 amount fractions due to inorganic processes were then calculated by subtracting this value from the observed $\Delta y(CO_2)$. Figure 10a shows the results for the vertical profiles on 2 August 2005. Figure 10a indicates that soil respiration was the main cause of the changes of CO_2 amount fractions, and the ER_{SA} of 1.12 ± 0.00 observed on the same day agreed with the OR of 1.1 for soil respiration. Figure 10b, however, shows substantial uptake of CO_2 by abiotic inorganic processes in the vertical profiles on 23 August 2005. The ER_{SA} of 1.25 ± 0.01 that was observed on the same day was clearly higher than the OR of 1.1. In addition, the higher SWC on 23 August (41.4 %) than on 2 August 2005 (31.0 %) suggested an influential effect of CO_2 dissolution on the substantial abiotic contributions on 23 August. In Sect 3.3, we separate the soil–air CO_2 fluxes observed at TKY, TKB, and MYK into the contributions from soil respiration and abiotic inorganic processes.

https://doi.org/10.5194/egusphere-2026-2751
Preprint. Discussion started: 16 June 2026

We next examine the relationships of the observed ER_{SA} at TKB with the O_2 and CO_2 amount fractions in soil pore air and SWC. We used the O_2 and CO_2 amount fractions in soil pore air to calculate the contribution of inorganic processes, which we equated to $\Delta y(CO_2) - (-\Delta y(O_2)(0.76)^{-1}(1.1)^{-1})$ based on the same rationale discussed above for TKY. Here, Δ denotes the differences of the CO_2 and O_2 amount fractions calculated by subtracting their 5-day mean values from the 30-min mean values. Figure 11a shows the O_2 and CO_2 amount fractions, the contributions of inorganic processes, the ER_{SA}, and the SWC for a period of 2.5 days beginning at 06:00 (JST) on 27 November 2024. This example is a typical case where the ER_{SA} exceeded 1.1. The water vapor in soil pore air makes the measured CO_2 and O_2 amount fractions lower than those in dry air. For example, the O_2 and CO_2 amount fractions of 20.94 % and 0.0450 % in dry air became 20.29 % and 0.0436 %, respectively, when the H_2O amount fraction was 3.1 % at a dew point of 25 °C. The CO_2 and O_2 amount fractions shown in Fig. 11a should therefore be corrected slightly when used to compare with the $\delta(O_2/N_2)$ and CO_2 amount fractions at TKY.

It is apparent from Fig. 11a that variations of the amount fractions were much larger for O_2 than CO_2. The implication is that the contribution of abiotic inorganic processes was substantial. The contribution of inorganic processes was negative when the ER_{SA} exceeded zero. The implication is that inorganic processes acted as a CO_2 sink relative to the average conditions 2.5 days before and after estimation of the ER_{SA}. Figure 11b shows the data from 29 April 2025 similar to those shown in Fig. 11a as an example of a typical case in which the ER_{SA} was less than 1.1. In this example, the contribution of inorganic processes was substantial, as in Fig. 11a, but inorganic processes acted as a CO_2 source rather than a sink relative to the average conditions 2.5-days before and after estimation of the ER_{SA}. The fact that the SWC was apparently higher in Fig. 11a than in Fig. 11b suggests that there was a close relationship among ER_{SA}, inorganic processes, and SWC.

Figure 11c shows the relationship between the ER_{SA} and the contribution of inorganic processes during the period November 2024 to October 2025 for the two main plots where crushed basalt was or was not spread. The ER_{SA} and SWC were clearly higher when inorganic processes acted as a CO_2 sink (e.g., Fig. 11a), except for two data points shown by light blue markers. The relationship among ER_{SA}, SWC, and the extent to which inorganic processes acted as a CO_2 sink suggests that the main contributor to the inorganic processes was dissolution of CO_2 in the soil water. Two exceptional data were recorded on 15 April 2025, when the CO_2 amount fraction was higher at a depth of 10 cm than at 65 cm. This difference may have been caused by desorption of CO_2 from near-surface soil due to the increase of temperature in spring. Such desorption may occur in the volcanic ash soil at TKB (Tabata et al., 2025a, b). This hypothesis is consistent with the fact that the three highest values of ER_{SA} were recorded on 28 November 2024 and 16 June 2025, within several weeks after tillage. The increase of the porosity of the soil by tillage increases the adsorption of CO_2. The implication is that the large variations of the ER_{SA} at TKB can be attributed not only to the effect of CO_2 dissolution but also to the effects of CO_2 adsorption and desorption in soil. We also examined the relationship between the ER_{SA} and SWC at MYK, but we found no correlation between them. The implication is that we need to consider an additional inorganic process to interpret the variations of the ER_{SA} at MYK.

https://doi.org/10.5194/egusphere-2026-2751
Preprint. Discussion started: 16 June 2026

3.3 Soil respiration and abiotic CO_2 fluxes estimated separately from the observed ER_{SA} and soil–air CO_2 flux

Figure 12a shows the seasonal variations of F_{CO2}, F_{CO2_R}, and F_{CO2_I} at TKY, TKB, and MYK. The F_{CO2}, F_{CO2_R}, and F_{CO2_I} are the observed soil–air CO_2 fluxes, and the contributions of soil respiration and inorganic processes, respectively, calculated from the method described in Sect. 2.4. Positive values indicate that the soil emits CO_2 to the atmosphere. It is clearly apparent from Fig. 12a that F_{CO2} at TKY and TKB underwent seasonal variations with summertime maxima. The absence of a similar seasonality at MYK may be related to the different climates at the three sites. The values of F_{CO2} of about 4 gC m^{-2} day^{-1} at TKY during the summer are consistent with those reported in our previous study at TKY (fig. 4 in Ishidoya et al., 2015). The F_{CO2} values were driven almost entirely by F_{CO2_R} at TKY. The seasonal variation of F_{CO2} at TKB was driven mainly by F_{CO2_R} as well, but substantial variations of F_{CO2_I} were occasionally observed. The variations of F_{CO2_I} are likely to be caused by the effect of dissolution of CO_2 in soil water and the effects of adsorption/desorption of CO_2 in soil, as discussed in Sect. 3.2. In contrast, both F_{CO2_R} and F_{CO2_I} contributed substantially to F_{CO2} at MYK, and the F_{CO2_I} values were negative during most of the observation period. Because no significant correlation was found between the ER_{SA} and SWC at MYK, the negative F_{CO2_I} could not be explained by the effect of dissolution of CO_2 in near-surface soil water. Alternatively, we hypothesize that the negative F_{CO2_I} is attributable to a combination of the effects of dissolution of CO_2 in soil water, weathering of calcium carbonate, and substantial percolation of soil water into groundwater at MYK. The argillic, calcareous, dark red soil at MYK is rich in calcium carbonate as well as in bicarbonate ions produced by Eqs. (11) and (12), and the soil water percolates into the ground rapidly because of the low water-holding capacity of the dark red soil and highly permeable Ryukyu limestone bedrock at MYK. The whole island of MYK may therefore act as a net CO_2 sink.

We also evaluated the effect of ERW by comparing F_{CO2_I} in the plots on which no mafic rock was spread (hereafter referred to as "control" plots) and the plots on which crushed basalt or olivine had been spread (hereafter referred to as "basalt" or "olivine" plots). The F_{CO2} values were higher in the control plot at TKB than in the basalt plot, especially in summer (Fig. 12a). A comparison of F_{CO2} with F_{CO2_R} and F_{CO2_I} revealed that F_{CO2_R} mainly accounted for the reduction of F_{CO2} in the basalt plot; in other words, soil respiration was suppressed by spreading crushed basalt. Seasonal differences of F_{CO2} between the control plot and basalt/olivine plots were not apparent at MYK, and both F_{CO2_R} and F_{CO2_I} contributed to the differences of F_{CO2}.

Figure 12b shows the average values of F_{CO2}, F_{CO2_R}, and F_{CO2_I} throughout the observation periods. We averaged the data at TKB during times when observations from both the control and basalt plots were available. Both F_{CO2} and F_{CO2_R} showed similar average values at TKY and TKB, whereas the average value of F_{CO2} was lower at MYK. The average F_{CO2_I} at both TKY and TKB did not differ significantly from zero, but it was significantly negative at MYK. It is clearly apparent from Fig. 12b that the differences between the average values of F_{CO2} in the control plots and basalt or olivine plots were due mainly to the corresponding differences between the average values of F_{CO2_R}. No significant differences were consequently found between the values of F_{CO2_I} in the control and basalt or olivine plots at TKB and MYK. There has hence been no evidence of a significant effect of ERW on F_{CO2} to date. In contrast, Beerling et al. (2024) have reported that ERW is likely to be associated

https://doi.org/10.5194/egusphere-2026-2751
Preprint. Discussion started: 16 June 2026

with a carbon dioxide removal (CDR) rate of 3.4 $tCO_2\ ha^{-1}\ year^{-1}$. The F_{CO2_I} corresponding to the CDR rate reported by Beerling et al. (2024) is also plotted in Fig. 12b (green line) and is comparable to the F_{CO2_I} at MYK. We could therefore detect the F_{CO2_I} due to ERW if the CDR was high, as reported by Beerling et al. (2024). Some recent studies have suggested that there has been an overestimation of the traditional model-based CDR rate of ERW and/or difficulty of its measurement, reporting, and verification (MRV) (e.g., Holden et al., 2024; Bertagni et al., 2024; Power et al., 2025). Because overestimation could lead to meaningless counting of carbon credits, reliable methods are indispensable for the MRV of the rate of CDR-associated ERW. The method developed in the present study, which enabled us to estimate F_{CO2_I} from precise soil–air O_2 and CO_2 fluxes, will be a promising tool for such MRV. For example, Ishidoya et al. (2024) have extracted the CO_2 emissions from a cement plant due only to the production of CaO from $CaCO_3$ (i.e., $CaCO_3 \rightarrow CaO + CO_2$) based on measurements of atmospheric $\delta(O_2/N_2)$ and CO_2 amount fractions. The method of Ishidoya et al. (2024) is considered applicable to estimation of CO_2 capture from flue gas or direct air capture. We therefore expect that simultaneous observations of $\delta(O_2/N_2)$ and CO_2 amount fractions will facilitate MRV of CDR techniques.

3.4 Isotopic effects of soil respiration and its implications for the Dole–Morita effect

Figure 13 shows the relative changes of $ln\,R/R_0$ as a function of $-lnf$ at TKY, TKB, and MYK obtained by applying the Rayleigh distillation equation (see Sect. 2.5). The plotted data were calculated from the $\delta_{atm}(^{18}O)$ versus $\delta(O_2/N_2)$ data in Figs. 3b, 4b, and 5b with r^2 values exceeding 0.5 for the relationship between $\delta_{atm}(^{18}O)$ and $\delta(O_2/N_2)$. The data observed at TKB on 28 November 2024 as well as 15 and 16 July 2025 for which the F_{CO2_I} values in Fig. 12a were notably high or low were also excluded to enable discussion of the ε_{SR} under average field conditions. The $ln\,R/R_0$ increased with increasing $-lnf$ at all sites (Fig. 13). The $\delta_{atm}(^{18}O)$ therefore increased as $\delta(O_2/N_2)$ decreased. The ε_{SR} values were estimated to be 14.7 ‰ ± 0.5 ‰, 6.9 ‰ ± 0.9 ‰, and 7.1 ‰ ± 1.4 ‰ at TKY, TKB, and MYK, respectively.

The ε_{SR} of 14.7 ‰ ± 0.5 ‰ at TKY was close to the global average ε_{SR} of 15.8 ‰ reported by Luz and Barkan (2011), rather than the ε_{SR} of 18 ‰ reported by Bender et al. (1994). The ε_{SR} reported by Luz and Barkan (2011) was taken from Angert et al. (2003), who reported ε_{SR} values of 10.1 ‰ ± 1.5 ‰, 17.8 ‰ ± 1.0 ‰, and 22.5 ‰ ± 3.6 ‰, in tropical, temperate, and boreal forests, respectively. TKY is located in a temporal deciduous forest, and the site's ε_{SR} was lower than that for temperate forests reported by Angert et al. (2003). Angert and Luz (2001) have reported ε_{SR} values of 11.9 ‰ to 20.0 ‰ (14.5 ‰ on average) based on closed-system incubation experiments for root respiration, and Angert et al. (2001) have reported an ε_{SR} of 12 ‰ ± 1 ‰ obtained from soil O_2 and $\delta_{atm}(^{18}O)$ profiles in the coastal plain of Israel. The ε_{SR} at TKY fell within the range of values reported by Angert and Luz (2001) and Angert et al. (2001). In contrast, the ε_{SR} values of 6.9 ‰ ± 0.9 ‰ and 7.1 ‰ ± 1.4 ‰ at TKB and MYK, respectively, were substantially lower than every ε_{SR} reported by Angert et al. (2001, 2003) and Angert and Luz (2001).

https://doi.org/10.5194/egusphere-2026-2751
Preprint. Discussion started: 16 June 2026

Angert et al. (2003) have found that the ε_{SR} in tropical, temperate, and boreal forests decreases with increasing soil temperature. The increase of the rate of soil respiration with increasing soil temperature lowers the O_2 amount fraction in soil air. An internal O_2 amount fraction that is lower than that of ambient air will decrease the ε_{SR} according to the diffusion–respiration model of Farquhar et al. (1982) (see Sect. 2.5). If we substitute the ε_{SR} of 14.7 ‰ ± 0.5 ‰ at TKY or 6.9 ‰ ± 0.9 ‰ at TKB for D_{total} and assume the D_d and D_r to be 0 ‰ and 18 ‰, respectively, then the C_i/C_a values are calculated to be 0.82 ± 0.03 for TKY and 0.38 ± 0.05 for TKB following the model. The implication is that the ε_{SR} at TKY and TKB were reduced from 18 ‰ because of the limiting effects of diffusion, which lowered the internal O_2 amount fraction to 82 % ± 3 % and 38 % ± 5 %, respectively, of the ambient O_2 amount fraction. The C_i/C_a ratio at TKB was not only lower than that at TKY but also lower than the ratio of 0.56 ± 0.08 calculated by substituting the average ε_{SR} of 10.1 ‰ ± 1.5 ‰ in a tropical forest (Angert et al., 2003) for D_{total} in Eq. (9). In general, the O_2 amount fraction in soil pore air tends to be lower in an agricultural field than in a forest because of the lower porosity of the soil, enhanced rate of decomposition of organic matter, and oxygen deficiency caused by irrigation. Such characteristics are a possible cause of the lower C_i/C_a ratios in agricultural fields.

Figure 14 shows the relationships between the ε_{SR} and O_2 amount fractions in soil pore air at TKY and TKB. The ε_{SR} at MYK is not shown in Fig. 14 because of the lack of data on O_2 amount fractions. The corresponding relationships for boreal forests, temperate forests, tropical forests, Mediterranean woodland, and tropical shrub land reported by Angert et al. (2003) are also plotted in Fig. 14. It is apparent from Fig. 14 that the ε_{SR} values decreased with decreasing O_2 amount fractions in soil pore air, except for the tropical shrub land. The implication is that the lower C_i/C_a is the cause of the lower ε_{SR} (vide supra), but further study is needed to interpret the exceptional case of the tropical shrub land. The global average ε_{SR} of 15.8 ‰ reported by Luz and Barkan (2011), calculated based on the observational results of Angert et al. (2003), is expected to be revised in light of our results. Specifically, the average ε_{SR} for temperate forests is lowered slightly by considering the smaller ε_{SR} of 14.7 ‰ ± 0.5 ‰ at TKY than the ε_{SR} of 17.8 ‰ ± 1.0 ‰ for temperate forests reported by Angert et al. (2003). The ε_{SR} in the agricultural fields at TKB and MYK, which are lower than all the ε_{SR} values reported by Angert et al. (2003), should also be considered.

If we assume that 12 % of the global land surface is represented by cultivated cropland (e.g., Cao et al. 2026) and that its ε_{SR} is equal to the value of 6.9 ‰ ± 0.9 ‰ measured at TKB, then the global average ε_{SR} is revised to 14.7 ‰ ($0.12 \times 6.9 + (1 - 0.12) \times 15.8$). The ε_{SR} for temperate forests would also be revised to 16.8 ‰, which is calculated by averaging the values of 14.8 ‰ at TKY and those of 17.8 ‰ and 17.9 ‰ in temperate forests reported by Angert et al. (2003). Because temperate forests represent about 16 % of global forests (Hansen et al., 2010), the global average ε_{SR} should be lowered by about 0.1 ‰ ($(17.8 - 16.8) \times 0.16 \times (1 - 0.12)$). The plausible global average ε_{SR} is therefore 14.6 ‰ based on an analysis that integrates the data from this study and that of Angert et al. (2003). If we use the ε_{SR} of 14.6 ‰ instead of the previous 15.8 ‰, then the steady-state Dole–Morita effect is revised from 23.16 ‰ to 22.71 ‰ based on the budgets and isotopic effects of atmospheric O_2 summarized in Luz and Barkan (2011). This revision amplifies the discrepancy with the observed Dole–Morita effect of 23.88 ‰ reported by Barkan and Luz (2005). Further studies are therefore needed to clarify the global O_2 budget and its

https://doi.org/10.5194/egusphere-2026-2751
Preprint. Discussion started: 16 June 2026

isotopic effects to deepen understanding of the Dole–Morita effect and its spatiotemporal variations (e.g., Bender et al., 1994; Luz and Barkan, 2011; Hoffmann et al., 2004; Ishidoya et al., 2025).

4 Conclusions

We conducted soil chamber measurements in a forest at TKY from February 2019 to August 2025, in agricultural fields at TKB from November 2024 to October 2025, and in agricultural fields at MYK from July 2023 to January 2026. The air samples we collected were analyzed for $\delta(O_2/N_2)$, CO_2 amount fraction, and $\delta_{atm}(^{18}O)$, and the thermally diffusive fractionation superimposed on the measured values was collected by using simultaneously measured $\delta(Ar/N_2)$ values. The average ER_{SA} of 1.101 ± 0.006 found at TKY agreed with the average ER_{SA} of 1.107 ± 0.010 observed by soil chamber measurements at TKY during 2004–2006 and 2011–2012 reported by Ishidoya et al. (2013a). The ER_{SA} at TKY varied slightly with the seasons and reached a seasonal maximum in June. The positive correlations that were found between SWC and both ER_{SA} and ER_{soil} suggested that CO_2 dissolution in soil water lowered the CO_2 amount fractions in soil pore air and led to the seasonal variations of ER_{SA}. ER_{SA} varied from 0.38 to 4.32 and from 0.82 to 3.35 at TKB and MYK, respectively. The close relationships also found at TKB among ER_{SA}, SWC, and the contribution of inorganic processes suggested that the large variations of ER_{SA} at TKB were due not only to the effect of CO_2 dissolution but also to the effects of CO_2 adsorption/desorption in soil.

We proposed a method to evaluate the contributions of soil respiration (F_{CO2_R}) and inorganic processes (F_{CO2_I}) to the soil–air CO_2 flux (F_{CO2}) separately, by assuming that the ER for F_{CO2} and F_{O2} due only to soil respiration was 1.1. The F_{CO2} values at TKY were driven almost entirely by F_{CO2_R}. The variation of F_{CO2} at TKB was also driven mainly by F_{CO2_R}, but substantial F_{CO2_I} variations were occasionally observed. However, both F_{CO2_R} and F_{CO2_I} contributed to F_{CO2} at MYK, and most of the F_{CO2_I} values were negative. The negative F_{CO2_I} values may be attributable to an eclectic process involving CO_2 dissolution, weathering of calcium carbonate, and substantial percolation into groundwater due to the low water-holding capacity of the soil at MYK. We evaluated the effect of ERW at TKB and MYK by comparing the F_{CO2_I} observed in the control and basalt/olivine plots. The F_{CO2} values were higher in the control plot at TKB than in the basalt plot, especially during summer. We estimated the main cause of the difference to be suppression of soil respiration in the basalt plot based on a comparison of F_{CO2}, F_{CO2_R}, and F_{CO2_I}. The average F_{CO2_I} at TKY and TKB did not differ significantly from zero, but it was negative at MYK. No significant differences were found between the F_{CO2_I} values in the control and basalt or olivine plots at TKB and MYK. We therefore did not observe a significant contribution of ERW to F_{CO2} at TKB and MYK. Nevertheless, the negative value of the average F_{CO2_I} at MYK was comparable to the CDR rate of 3.4 $tCO_2\ ha^{-1}\ year^{-1}$ expected from ERW (Beerling et al., 2024). The implication is that the method to estimate F_{CO2_I} proposed in the present study is a promising tool for the MRV of the rate of CDR due to ERW.

The $\delta_{atm}(^{18}O)$ and $\delta(O_2/N_2)$ data observed at TKY, TKB, and MYK were used to estimate ε_{SR} by applying the Rayleigh distillation equation. The ε_{SR} values were estimated to be 14.7 ‰ ± 0.5 ‰, 6.9 ‰ ± 0.9 ‰, and 7.1 ‰ ± 1.4 ‰ at TKY, TKB, and MYK, respectively. The value of the ε_{SR} at TKY was between the values of 10.1 ‰ ± 1.5 ‰ and 17.8 ‰ ± 1.0 ‰ observed

https://doi.org/10.5194/egusphere-2026-2751
Preprint. Discussion started: 16 June 2026

in tropical and temperate forests, respectively, by Angert et al. (2003). In contrast, the ε_{SR} values at TKB and MYK were substantially lower than every ε_{SR} reported by Angert et al. (2001, 2003) and Angert and Luz (2001). A relatively low ε_{SR} suggests a relatively low internal O_2 amount fraction of the oxygen consumed in the soil based on the diffusion–respiration model of Farquhar et al. (1982). This scenario is supported by the positive correlation between the ε_{SR} and O_2 amount fraction in soil pore air, which was revealed by the observations in this study and those of Angert et al. (2003), with the exception of tropical shrub land. We revised the global average ε_{SR} to 14.6 ‰ from the value of 15.8 ‰ reported by Luz and Barkan (2011) based on an analysis that integrated the ε_{SR} values reported in this study and those of Angert et al. (2003). The steady state Dole–Morita effect of 23.16 ‰, which was calculated from O_2 budgets and isotopic effects summarized in Luz and Barkan (2011), was then revised to 22.71 ‰. Because the observed Dole–Morita effect is 23.88 ‰ (Barkan and Luz, 2005), the inconsistency between the observed and modeled Dole–Morita effect was increased by the revision.

In conclusion, we confirmed that precise values of $\delta(O_2/N_2)$, CO_2 amount fractions, and $\delta_{atm}(^{18}O)$ obtained from soil chamber measurements are valuable not only for separation of the contributions of F_{CO2_R} and F_{CO2_I} to F_{CO2}, which will be a promising tool for the MRV of ERW, but also for determination of reliable values of ε_{SR} to evaluate changes of the Dole–Morita effect, which provides information about the global cycles of oxygen, carbon, and water. However, only a few studies have reported precise values of $\delta(O_2/N_2)$ from soil chamber measurements, and the present study is the only one to report $\delta_{atm}(^{18}O)$. More observations are therefore needed to clarify the spatiotemporal variations of F_{CO2_R}, F_{CO2_I}, and ε_{SR} ranging from agricultural-field scales to global scales.

Data availability The $y(CO_2)$, $\delta(O_2/N_2)$, and $\delta_{atm}(^{18}O)$ data from soil chamber measurements at TKY, TKB, and MYK, and the $y(CO_2)$ and $\Delta y(O_2)$ in soil pore air at TKY are included as electronic supplement to the paper.

Author contributions SI designed the study; conducted soil chamber measurements at TKY, TKB, and MYK; measured $\delta(O_2/N_2)$, CO_2 amount fractions, $\delta_{atm}(^{18}O)$, $\delta_{atm}(^{15}N)$, and $\delta_{atm}(^{40}Ar)$ for the collected air samples; and drafted the manuscript. SI also conducted $\delta(O_2/N_2)$ measurements of soil pore air at TKY. MT and AY supported design of the experimental procedures of soil chamber measurements at TKB and MYK. KH and SSuzuki managed the MYK agricultural fields and conducted SWC measurements. JF, IS, SE, RW, KA, TN, and TY managed the TKB agricultural fields and conducted measurements of CO_2 and O_2 amount fractions in soil pore air and SWC. SM managed the TKY forest site and conducted soil pore air sampling and SWC measurements. AH analyzed the SWC at TKY. SSugawara examined the discussion regarding $\delta_{atm}(^{18}O)$. SA and TN managed measurement systems at Tohoku University. All authors provided feedback on the manuscript and approved the final manuscript.

Competing interests The authors declare that they have no conflict of interest.

https://doi.org/10.5194/egusphere-2026-2751
Preprint. Discussion started: 16 June 2026

Acknowledgements We acknowledge K. Kurumado, S. Yoshitake, K. Suzuki, and H. Hiratsuka, as well as members of the River Basin Research Center of Gifu University for their cooperation. We thank the field technicians at NIAES-NARO for their support in maintaining the field experiment at TKB. We would also like to thank C. Takamura of Tohoku University (currently at C. Sawada of National Institute for Environmental Studies) for the soil pore air sampling at TKY and subsequent measurements of CO_2 amount fractions.

Financial support This study was supported by the NEDO Moonshot Research and Development Program (Grant number: P18016), Japan Society for the Promotion of Science KAKENHI (grant nos. 22H05006, 18H03365, and 22H00564), and the Global Environment Research Coordination System from the Ministry of the Environment, Japan (grant nos. METI1953 and MAFF2254).

References

Angert, A., Luz, B., and Yakir, D.: Fractionation of oxygen isotopes by respiration and diffusion in soils: Implications for the isotopic composition of atmospheric O_2, Global Biogeochem. Cy., 15, 871–881, https://doi.org/10.1029/2000GB001371, 2001.

Angert, A., and Luz, B.: Fractionation of oxygen isotopes by root respiration: Implications for the isotopic composition of atmospheric O_2, Geochim. Cosmochim. Acta, 65, 1695–1701, https://doi.org/10.1016/S0016-7037(01)00567-1,2001.

Angert, A., Barkan, E., Barnett, B., Brugnoli, E., Davidson, E. A., Fessenden, J., Maneepong, S., Nipa Panapitukkul, N., Randerson, J. T., Savage, K., Yakir, D., and Luz, B.: The contribution of soil respiration in tropical, temperate, and boreal forests to the ^{18}O enrichment of atmospheric O_2, Global Biogeochem. Cycles, 17(3), 1089, doi:10.1029/2003GB002056, 2003.

Angert, A., Yakir, D., Rodeghiero, M., Preisler, Y., Davidson, E. A., and Weiner, T.: Using O_2 to study the relationships between soil CO_2 efflux and soil respiration, Biogeosciences, 12, 2089–2099, https://doi.org/10.5194/bg-12-2089-2015, 2015.

Aoki, N., Ishidoya, S., Matsumoto, N., Watanabe, T., Shimosaka, T., and Murayama, S.: Preparation of primary standard mixtures for atmospheric oxygen measurements with less than 1 μmol mol^{-1} uncertainty for oxygen molar fractions, Atmos. Meas. Tech., 12, 2631–2646, https://doi.org/10.5194/amt-12-2631-2019, 2019.

Aoki, N., Ishidoya, S., Tohjima, Y., Morimoto, S., Keeling, R. F., Cox, A., Takebayashi, S., and Murayama, S.: Intercomparison of O_2/N_2 ratio scales among AIST, NIES, TU, and SIO based on a round-robin exercise using gravimetric standard mixtures, Atmos. Meas. Tech., 14, 6181–6193, https://doi.org/10.5194/amt-14-6181-2021, 2021.

Armstrong, W., Strange, M. E., Cringle, S., and Beckett, P. M.: Microelectrode and modelling study of oxygen distribution in roots, Ann. Bot., 74(3), 287–299, 1994.

https://doi.org/10.5194/egusphere-2026-2751
Preprint. Discussion started: 16 June 2026

Barkan, E., and Luz, B.: High precision measurements of $^{17}O/^{16}O$and $^{18}O/^{16}O$ ratios in H_2O, Rapid Commun. Mass Spectrom., 24, 3737–3742, doi:10.1002/rcm.2250, 2005.

Battle, M. O., William Munger, J., Conley, M., Sofen, E., Perry, R., Hart, R., Davis, Z., Scheckman, J., Woogerd, J., Graeter, K., Seekins, S., David, S., and Carpenter, J.: Atmospheric measurements of the terrestrial O_2 : CO_2 exchange ratio of a midlatitude forest, Atmospheric Chemistry and Physics, 19, 8687–8701, https://doi.org/10.5194/acp-19-8687-2019, 2019.

Beerling, D. J., Kantzas, E. P., Lomas, M. R., Wade, P., Eufrasio, R. M., Renforth, P., Sarkar, B., Andrews, M. G., James, R. H., Pearce, C. R., Mercure, J. F., Pollitt, H., Holden, P. B., Edwards, N. R., Khanna, M., Koh, L., Quegan, S., Pidgeon, N. F., Janssens, I. A., Hansen, J., and Banwart, S. A.: Potential for large-scale CO_2 removal via enhanced rock weathering with croplands, Nature, 583, 242–248, https://doi.org/10.1038/s41586-020-2448-9, 2020.

Beerling, D. J., Epihov, D. Z., Kantola, I. B., Masters, M. D., Reershemius, T., Planavsky, N. J., Reinhard, C. T., Jordan, J. S., Thorne, S. J., Weber, J., Martin, M. V., Freckleton, R. P., Hartley, S. E., James, R. H., Pearce, C. R., DeLucia, E. H., and Banwart, S. A.: Enhanced weathering in the US Corn Belt delivers carbon removal with agronomic benefits, Proceedings of the National Academy of Sciences, 121(9), e2319436121. https://doi.org/10.1073/pnas.2319436121, 2024.

Bender, M., Sowers, T., and Labeyrie, L.: The Dole effect and its variations during the last 130,000 years as measured in the Vostok ice core, Global Biogeochem. Cycles, 8(3), 363–376, 1994.

Bertagni, M. B., Calabrese, S., Cipolla, G., Noto, L. V., and Porporato, A.: Advancing enhanced weathering modeling in soils: Critical comparison with experimental data, Journal of Advances in Modeling Earth Systems, 17, e2024MS004224. https://doi.org/10.1029/2024MS004224, 2024.

Cao, P., Bilotto, F., Fischer, C. G., Mueller, N. D., Carlson, K. M., Driscoll, A. W., Gerber, J. S., Smith, P., Tubiello, F. N., West, P. C., You, L., Herrero, M.: Spatially explicit global assessment of cropland greenhouse gas emissions circa 2020, Nat. Clim. Change, https://doi.org/10.1038/s41558-026-02558-4, 2026.

Cohen, E. R., Cvitas, T., Frey, J. G., Holmstrom, B., Kuchitsu, K., Marquardt, R., Mills, I., Pavese, F., Quack, M., Stohner, J., Strauss, H., Takami, M., and Thor, A. J.: IUPAC Green Book: 3rd edn., RSC Publishing, ISBN 0854044337, ISBN-13 9780854044337, 2007.

Dole, M.: The relative atomic weight of oxygen in water and in air, J. Am. Chem. Soc., 57, 2731, https://doi.org/10.1021/ja01315a511, 1935.

Faassen, K. A. P., Nguyen, L. N. T., Broekema, E. R., Kers, B. A. M., Mammarella, I., Vesala, T., Pickers, P. A., Manning, A. C., Vilà-Guerau de Arellano, J., Meijer, H. A. J., Peters, W., and Luijkx, I. T.: Diurnal variability of atmospheric O_2, CO_2, and their exchange ratio above a boreal forest in southern Finland, Atmos. Chem. Phys., 23, 851–876, https://doi.org/10.5194/acp-23-851-2023, 2023.

Farquhar, G. D., O'Leary, M. H., & Berry, J. A.: On the relationship between carbon isotope discrimination and the intercellular carbon dioxide concentration in leaves, Australian Journal of Plant Physiology, 9(2), 121–137, https://doi.org/10.1071/PP9820121, 1982.

https://doi.org/10.5194/egusphere-2026-2751
Preprint. Discussion started: 16 June 2026

Farquhar, G. D., & Lloyd, J.: Carbon and oxygen isotope effects in the exchange of carbon dioxide between terrestrial plants and the atmosphere. In Stable Isotopes and Plant Carbon-Water Relations (pp. 47–70), https://doi.org/10.1016/B978-0-08-091801-3.50011-8, 1993.

Guy, R. D., Berry, J. A., Fogel, M. L., and Hoering, T. C.: Differential fractionation of oxygen isotopes by cyanide-resistant and cyanide-sensitive respiration in plants, Planta, 177(4), 483–491, https://doi.org/10.1007/BF00392616, 1989.

Guy, R. D., Fogel, M. L., and Berry, J. A.: Photosynthetic fractionation of the stable isotopes of oxygen and carbon. Plant Physiology, 101(1), 37–47. https://doi.org/10.1104/pp.101.1.37, 1993.

Hansen, M. C., Stehman, S. V., and Potapov, P. V.: Quantification of global gross forest cover loss, PNAS, 107(19), 8650–8655, doi: 10.1073/pnas.0912668107, 2010.

Hilman, B., Weiner, T., Haran, T., Masiello, C. A., Gao, X., Angert, A.: The apparent respiratory quotient of soils and tree stems and the processes that control it, Journal of Geophysical Research: Biogeosciences, 127, e2021JG006676. https://doi. org/10.1029/2021JG006676, 2022.

Hoffmann, G., Suntz, M., Weber, C., Ciais, P., Friedlingstein, P., Heimann, M., Jouzel, J., Kaduk, J., Maier-Reimer, E., Seibt, U., and Six, K.: A model of the Earth's Dole effect, Global Biogeochem. Cycles, 18, GB1008, doi:10.1029/2003GB002059, 2004.

Holden, F. J., Davies, K., Bird, M. I., Hume, R., Green, H., Beerling, D. J., & Nelson, P. N.: In-field carbon dioxide removal via weathering of crushed basalt applied to acidic tropical agricultural soil, Sci. Total Environ., 955, 176568, https://doi.org/10.1016/j.scitotenv.2024.176568, 2024.

Ishidoya, S., Aoki, S. and Nakazawa, T.: High precision measurements of the atmospheric O_2/N_2 ratio on a mass spectrometer. J. Meteorol. Soc. Jpn. 81, 127–140, 2003.

Ishidoya, S., Murayama, S., Takamura, C., Kondo, H., Saigusa, N., Goto, D., Morimoto, S., Aoki, N., Aoki, S., and Nakazawa, T.: O_2:CO_2 exchange ratios observed in a cool temperate deciduous forest ecosystem of central Japan, Tellus B, 65, doi:10.3402/tellusb.v65i0.21120, 2013a.

Ishidoya, S., Sugawara, S., Morimoto, S., Aoki, S., Nakazawa, T., Honda, H., and Murayama, S.: Gravitational separation in the stratosphere – a new indicator of atmospheric circulation, Atmos. Chem. Phys., 13, 8787-8796, doi:10.5194/acp-13-8787-2013, 2013b.

Ishidoya, S., and Murayama, S.: Development of high precision continuous measuring system of the atmospheric O_2/N_2 and Ar/N_2 ratios and its application to the observation in Tsukuba, Japan, Tellus B, 66, 22574, http://dx.doi.org/10.3402/tellusb.v66.22574, 2014.

Ishidoya, S., Murayama, S., Kondo, H., Saigusa, N., Kishimoto-Mo, A. W., and Yamamoto, S.: Observation of O2 : CO2 exchange ratio for net turbulent fluxes and its application to forest carbon cycles, Ecol. Res., 30, 225–234, 2015.

Ishidoya, S., Sugawara, H., Terao, Y., Kaneyasu, N., Aoki, N., Tsuboi, K., and Kondo, H.: O_2 : CO_2 exchange ratio for net turbulent flux observed in an urban area of Tokyo, Japan, and its application to an evaluation of anthropogenic CO_2 emissions, Atmos. Chem. Phys., 20, 5293–5308, https://doi.org/10.5194/acp-20-5293-2020, 2020.

https://doi.org/10.5194/egusphere-2026-2751
Preprint. Discussion started: 16 June 2026

Ishidoya, S., Tsuboi, K., Niwa, Y., Matsueda, H., Murayama, S., Ishijima, K., and Saito, K.: Spatiotemporal variations of the $\delta(O_2/N_2)$, CO_2 and δ(APO) in the troposphere over the western North Pacific, Atmos. Chem. Phys., 22, 6953–6970, https://doi.org/10.5194/acp-22-6953-2022, 2022.

Ishidoya, S., Tsuboi, K., Kondo, H., Ishijima, K., Aoki, N., Matsueda, H., and Saito, K.: Measurement report: Method for evaluating CO_2 emissions from a cement plant using atmospheric $\delta(O_2/N_2)$ and CO_2 measurements and its implication for future detection of CO_2 capture signals, Atmos. Chem. Phys., 24, 1059–1077, https://doi.org/10.5194/acp-24-1059-2024, 2024.

Ishidoya, S., Sugawara, S. and Okazaki, A.; Diurnal, seasonal, and interannual variations in $\delta(^{18}O)$ of atmospheric O_2 and its application to evaluate natural and anthropogenic changes in oxygen, carbon, and water cycles, Atmos. Chem. Phys., 25, 1965–1987, https://doi.org/10.5194/acp-25-1965-2025, 2025.

Kato, T., Nakazawa, T., Aoki, S., Sugawara, S., and Ishizawa, M.: Seasonal variation of the oxygen isotopic ratio of atmospheric carbon dioxide in a temperate forest, Japan, Glob. Biogeochem. Cy., 18, GB2020, doi:10.1029/2003GB002173, 2004.

Kawamura, K., Nakazawa, T., Aoki, S., Sugawara, S., Fujii, Y., and Watanabe, O.: Atmospheric CO_2 variations over the last three glacial–interglacial climatic cycles deduced from the Dome Fuji deep ice core, Antarctica using a wet extraction technique, Tellus B, 55, 126–137, https://doi.org/10.3402/tellusb.v55i2.16730, 2003.

Keeling, R. F.: Development of an interferometric oxygen analyzer for precise measurement of the atmospheric O_2 mole fraction, Ph.D. thesis, Harvard University, Cambridge, 1988.

Kishimoto-Mo, A. W., Yonemura, S., Uchida, M., Kondo, M., Murayama, S., and Koizumi, H.: Contribution of soil moisture to seasonal and annual variations of soil CO_2 efflux in a humid cool-temperate oak-birch forest in central Japan, Ecol. Res., 30, 311-325, doi:10.1007/s11284-015-1254-6, 2015.

Kroopnick, P., and Craig, H.: Oxygen isotope fractionation in dissolved oxygen in the deep sea, Earth Planet. Sci. Lett., 32, 375–388, 1976.

Lee, M.-S., Nakane, K., Nakatsubo, T., and Koizumi, H.: The importance of root respiration in annual soil carbon fluxes in a cool-temperate deciduous forest, Agr. For. Meteorol., 134, 95-101. https://doi.org/10.1016/j.agrformet.2005.08.011, 2005.

Luz, B., and Barkan, E.: The isotopic composition of atmospheric oxygen, Global Biogeochem. Cycles, 25, GB3001, doi:10.1029/2010GB003883, 2011.

Manning, A. C. and Keeling, R. F.: Global oceanic and terrestrial biospheric carbon sinks from the Scripps atmospheric oxygen flask sampling network. Tellus B. 58, 95– 116, 2006.

Massman, W. J.: A review of the molecular diffusivities of H_2O, CO_2, CH_4, CO, O_3, SO_2, NH_3, N_2O, NO, and NO_2 in air, O_2 and N_2 near STP, Atmos. Environ., 32, 1111–1127, 1998.

Morita, N.: The increased density of air oxygen relative to water oxygen, J. Chem. Soc. Japan, 56, 1291, 1935.

https://doi.org/10.5194/egusphere-2026-2751
Preprint. Discussion started: 16 June 2026

Murayama, S., Kondo, H., Ishidoya, S., Maeda, T., Saigusa, N., Yamamoto, S., Kamezaki, K., and Muraoka, H.: et al. (2024). Interannual variation and trend of carbon budget observed for more than two decades at Takayama in a cool-temperate deciduous forest in central Japan, Journal of Geophysical Research: Biogeosciences, 129, e2023JG007769, https://doi.org/10.1029/2023JG007769, 2024.

Nakazawa, T., Aoki, S., Murayama, S., Fukabori, M., Yamanouchi, T., and Murayama, H.: The concentration of atmospheric carbon dioxide at Japanese Antarctic station, Syowa, Tellus B, 43, 126– 135, https://doi.org/10.3402/tellusb.v43i2.15257,1991.

Pickers, P. A., Manning, A. C., Le Quéré, C., Forster, G. L., Luijkx, I. T., Gerbig, C., Fleming, L. S., and Sturges, W. T.: Novel quantification of regional fossil fuel CO2 reductions during COVID-19 lockdowns using atmospheric oxygen measurements, Sci. Adv., 8, eabl9250, https://doi.org/10.1126/sciadv.abl9250, 2022.

Power, I. M., Hatten, V. N. J., Guo, M., Schaffer, Z. R., Rausis, K. and Klyn-Hesselink, H.: Are enhanced rock weathering rates overestimated? A few geochemical and mineralogical pitfalls, Front. Clim., 6:1510747.doi: 10.3389/fclim.2024.1510747, 2025.

Seibt, U.: Processes controlling the isotopic composition of CO_2 and O_2 in canopy air: A theoretical analysis with some observations in a Sitka spruce plantation, Ph.D. thesis, Universität Hamburg, Hamburg, 2003.

Seibt, U., Brand, W. A., Heimann, M., Lloyd, J., Severinghaus, J. P., Wingate, L.: Observations of O_2:CO_2 exchange ratios during ecosystem gas exchange, Glob. Biogeochem. Cy., 18:GB4024. doi:10.1029/2004GB002242, 2004.

Severinghaus, J.: Studies of the terrestrial O_2 and carbon cycles in sand dune gases and in biosphere 2, Ph. D. thesis, Columbia University, New York, 1995.

Sugawara, S., Ishidoya, S., Aoki, S., Morimoto, S., Nakazawa, T., Toyoda, S., Inai, Y., Hasebe, F., Ikeda, C., Honda, H., Goto, D., and Putri, F. A.: Age and gravitational separation of the stratospheric air over Indonesia, Atmos. Chem. Phys., 18, 1819–1833, https://doi.org/10.5194/acp-18-1819-2018, 2018.

Sugawara, H., Ishidoya, S., Terao, Y., Takane, Y., Kikegawa, Y., and Nakajima, K.: Anthropogenic CO_2 emissions changes in an urban area of Tokyo, Japan, due to the COVID-19 pandemic: A case study during the state of emergency in April–May 2020. Geophysical Research Letters, 48, e2021GL092600. https://doi. Org/10.1029/2021GL092600, 2021.

Tabata, S., and Yonemura, S.: Simulation of physical sorption of CO_2 of volcanic ash soil in closed-chamber methods. Journal of Agricultural Meteorology, 81(3), 147–151. https://doi.org/10.2480/agrmet.D-24-00037, 2025a.

Tabata, S., Yonemura, S., Wagai, R.: Adsorption and desorption of carbon dioxide by volcanic ash soil: quantitative analysis using the flow-through chamber method. Soil Science and Plant Nutrition, 1-8. https://doi.org/10.1080/00380768.2025.2496402, 2025b.

Tohjima, Y., Machida, T., Watai, T., Akama, I., Amari, T., and Moriwaki, Y.: Preparation of gravimetric standards for measurements of atmospheric oxygen and reevaluation of atmospheric oxygen concentration, J. Geophys. Res., 110, D1130, https://doi.org/10.1029/2004JD005595, 2005.

https://doi.org/10.5194/egusphere-2026-2751
Preprint. Discussion started: 16 June 2026

Tohjima, Y., Mukai, H., Machida, T., Hoshina, Y., and Nakaoka, S.-I.: Global carbon budgets estimated from atmospheric O_2/N_2 and CO_2 observations in the western Pacific region over a 15-year period, Atmos. Chem. Phys., 19, 9269–9285, https://doi.org/10.5194/acp-19-9269-2019, 2019.

Uchida, M., Mo, W., Nakatsubo, T., Tsuchiya, Y., Horikoshi, T., and Koizumi, H.: Microbial activity and litter decomposition under snow cover in a cool-temperate broad-leaved deciduous forest. Agricultural and Forest Meteorology, 134, 102-109, https://doi.org/10.1016/j.agrformet.2005.11.003, 2005.

Wagai, R., Kajiura, M., Uchida, M., and Asano, M.: Distinctive Roles of Two Aggregate Binding Agents in Allophanic Andisols: Young Carbon and Poorly-Crystalline Metal Phases with Old Carbon, Soil Syst., 2(2), 29, https://doi.org/10.3390/soilsystems2020029, 2018.

Wang, Z.-Y., Xie, J.-B., Wang, Y.-G., and Li, Y.: Biotic and abiotic contribution to diurnal soil CO_2 fluxes from saline/alkaline soils. Scientific Reports, 10, 5396. https://doi.org/10.1038/s41598-020-62209-2, 2020.

Worrall, F., Clay, G. D., Howden, N. J. K., and Burt, T. P: Chemical oxygen demand as a measure of fluvial organic matter oxidation state. Journal of Geophysical Research: Biogeosciences, 128, e2022JG007248, https://doi.org/10.1029/2022JG007248, 2023.

https://doi.org/10.5194/egusphere-2026-2751
Preprint. Discussion started: 16 June 2026

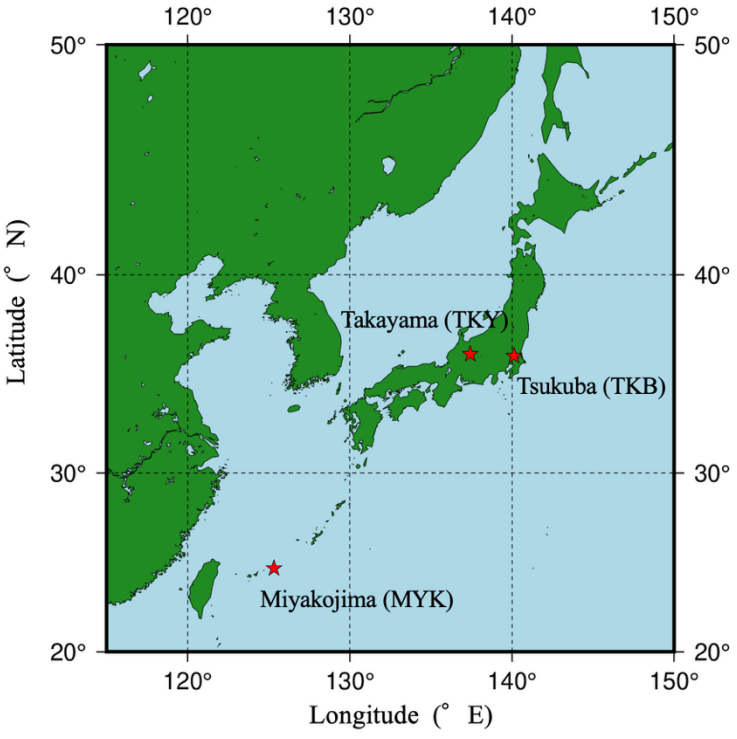

Figure 1. Location of the Takayama forest site (TKY), and the agricultural fields located in Tsukuba (TKB) and Miyakojima (MYK).

https://doi.org/10.5194/egusphere-2026-2751
Preprint. Discussion started: 16 June 2026

738
739

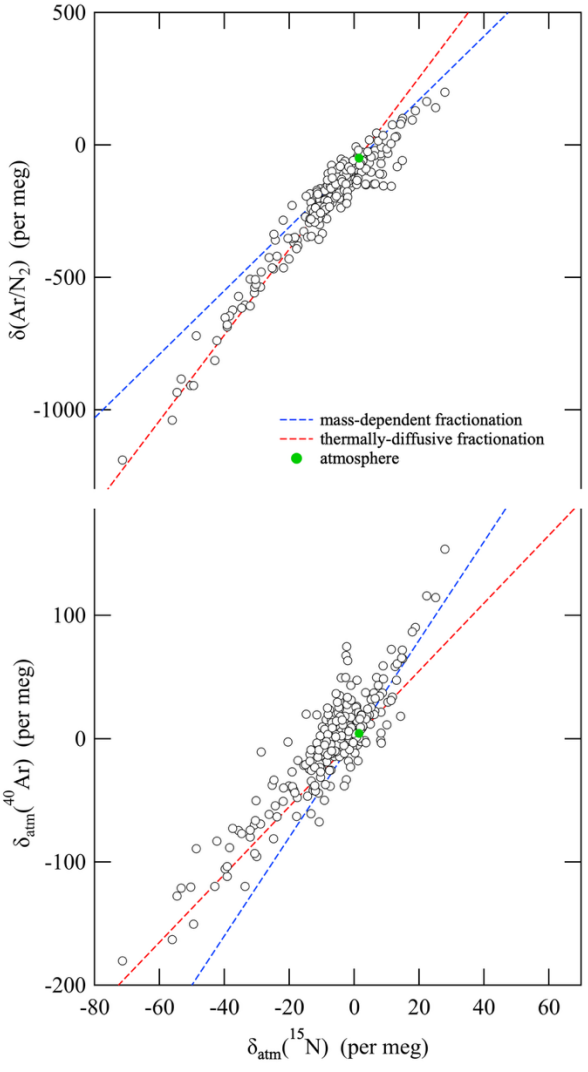

740

741 **Figure 2.** Measured $\delta(Ar/N_2)$ and $\delta_{atm}(^{40}Ar)$ plotted against $\delta_{atm}(^{15}N)$ for all the air samples collected via soil chamber experiments at TKY,
742 TKB, and MYK (black open circles). The relationships expected from mass-dependent (blue dashed lines) and thermally diffusive (red
743 dashed lines) fractionations of air molecules are also shown. Average atmospheric $\delta(Ar/N_2)$ and $\delta_{atm}(^{40}Ar)$ are indicated by green filled
744 circles.

745
746

https://doi.org/10.5194/egusphere-2026-2751
Preprint. Discussion started: 16 June 2026

747

748 (a)

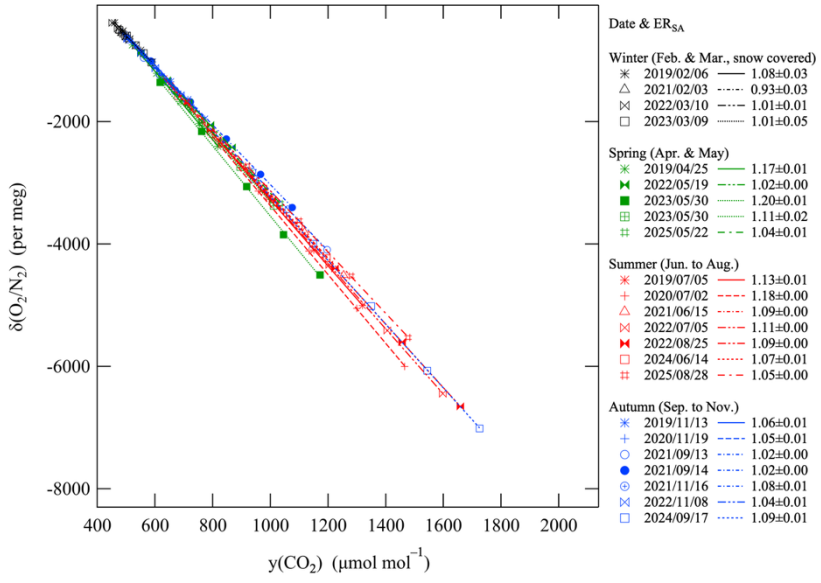

749

750 (b)

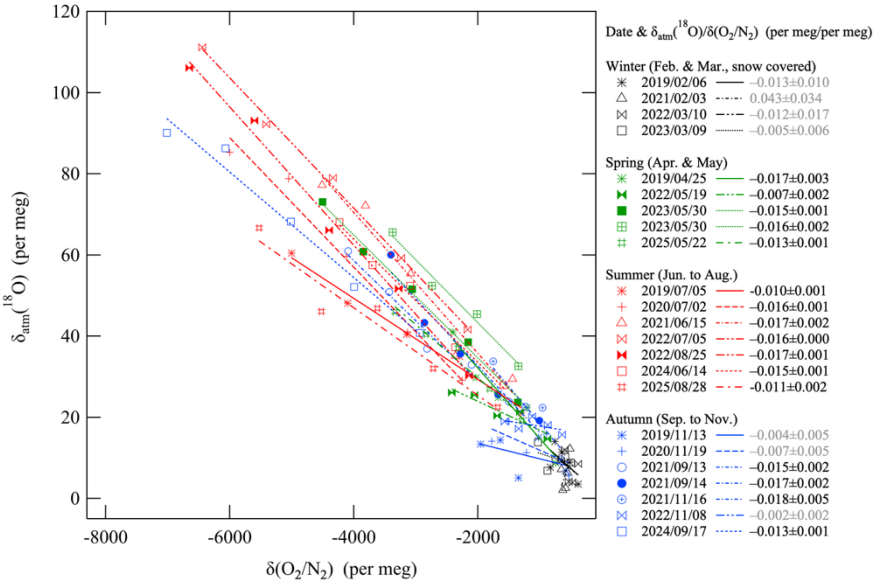

751

752 **Figure 3.** (a) Relationships between $\delta(O_2/N_2)$ and $y(CO_2)$ at TKY obtained from 23 soil chamber measurements from 6 February 2019 to 28
753 August 2025. Least-squares regression lines fitted to the data for the respective experiments are also shown. The *y* stands for the dry amount
754 fraction of gas recommended by the IUPAC Green Book. (b) Same as in (a) but for the relationship between $\delta_{atm}(^{18}O)$ and $\delta(O_2/N_2)$. Gray
755 text in legends denotes relationships with r^2 values lower than 0.5.

https://doi.org/10.5194/egusphere-2026-2751
Preprint. Discussion started: 16 June 2026

(a)

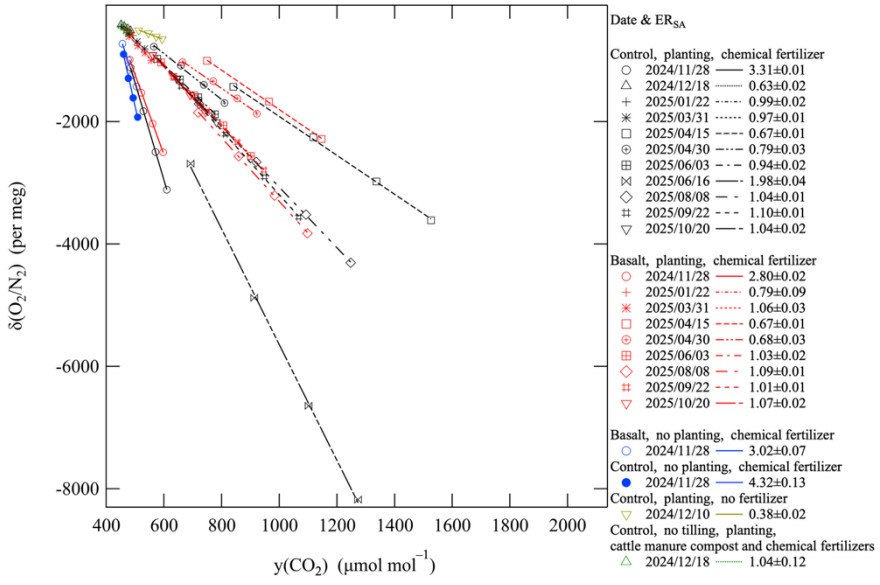

(b)

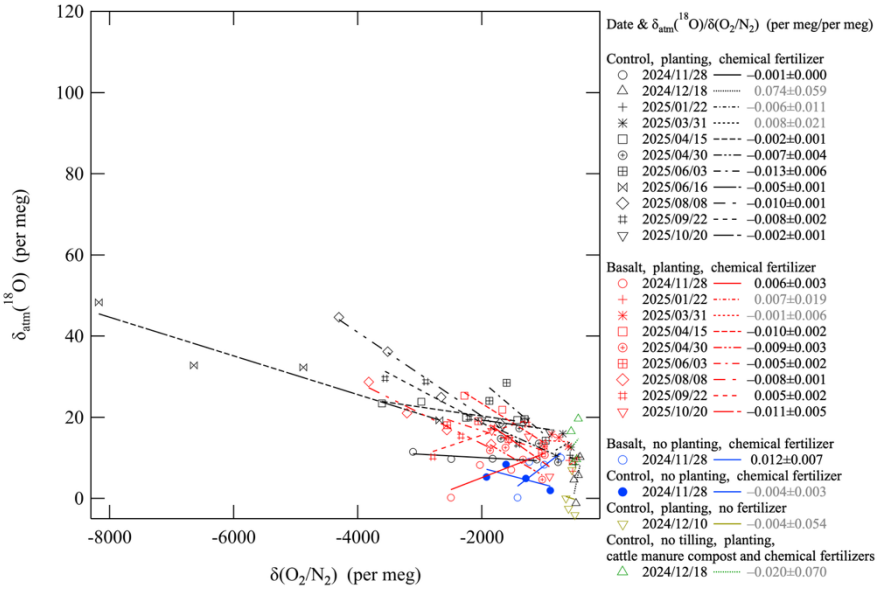

Figure 4. (a) Relationships between $\delta(O_2/N_2)$ and $y(CO_2)$ at TKB obtained from 24 soil chamber measurements during the period 28 November 2024 to 20 October 2025. Least-squares regression lines fitted to the data for the respective experiments are also shown. "Control" and "Basalt" denote the plots without and with application of crushed basalt, respectively. "Planting" denotes that soybeans (June–October)

https://doi.org/10.5194/egusphere-2026-2751
Preprint. Discussion started: 16 June 2026

and barley (November–May) were grown in the plots. See the text for details of the field conditions. (b) Same as in (a) but for the relationship between $\delta_{atm}(^{18}O)$ and $\delta(O_2/N_2)$. Gray text in legends denotes relationships with r^2 values lower than 0.5.

https://doi.org/10.5194/egusphere-2026-2751
Preprint. Discussion started: 16 June 2026

768

769 (a)

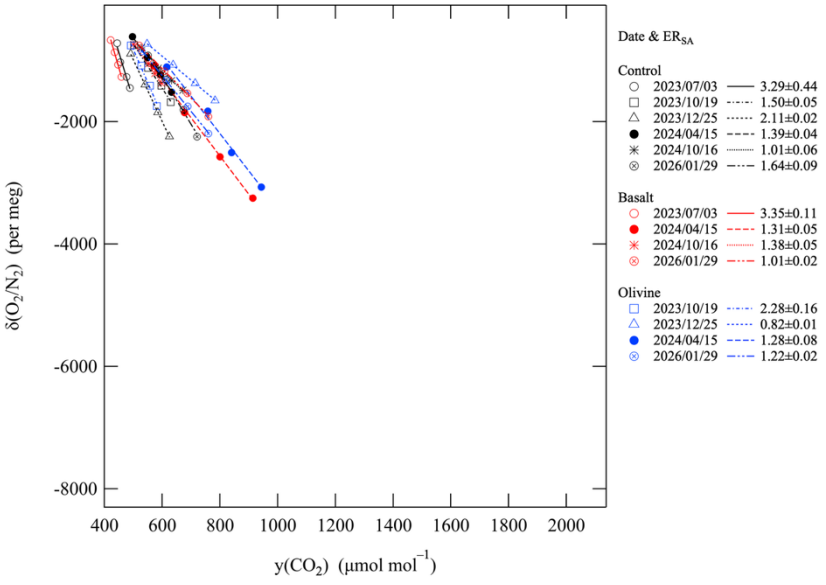

770

771 (b)

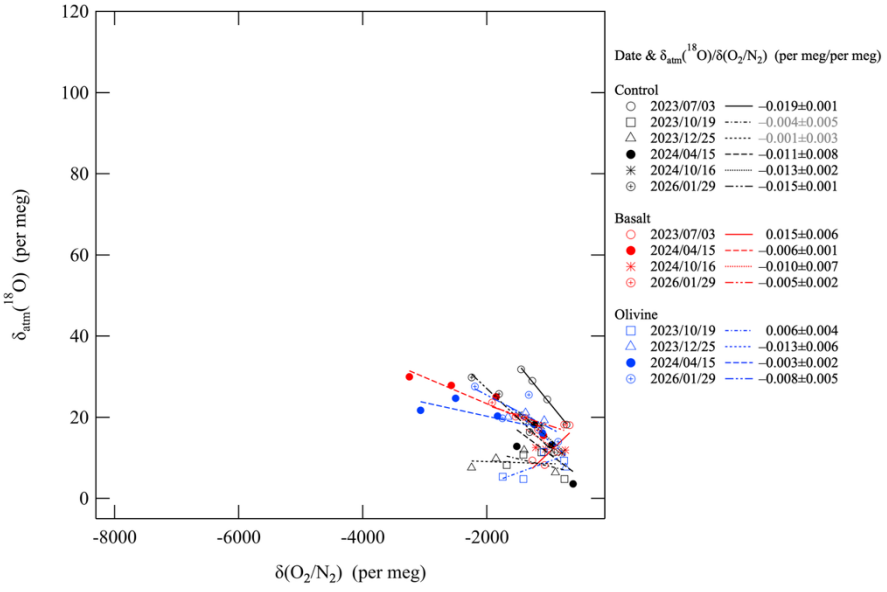

772

773 **Figure 5.** (a) Relationships between $\delta(O_2/N_2)$ and $y(CO_2)$ in the MYK agricultural field obtained from 14 soil chamber measurements during
774 the period 3 July 2023 to 29 January 2026. Least-squares regression lines fitted to the data for the respective experiments are also shown.
775 Yams were planted in the plots. "Control", "basalt", and "olivine" denote plots without application of crushed basalt/olivine, with application

https://doi.org/10.5194/egusphere-2026-2751
Preprint. Discussion started: 16 June 2026

of basalt, and with application of olivine, respectively. See the text for details of the field conditions. (b) Same as in (a) but for the relationship between $\delta_{atm}(^{18}O)$ and $\delta(O_2/N_2)$. Gray text in legends denotes relationships with r^2 values lower than 0.5.

https://doi.org/10.5194/egusphere-2026-2751
Preprint. Discussion started: 16 June 2026

781

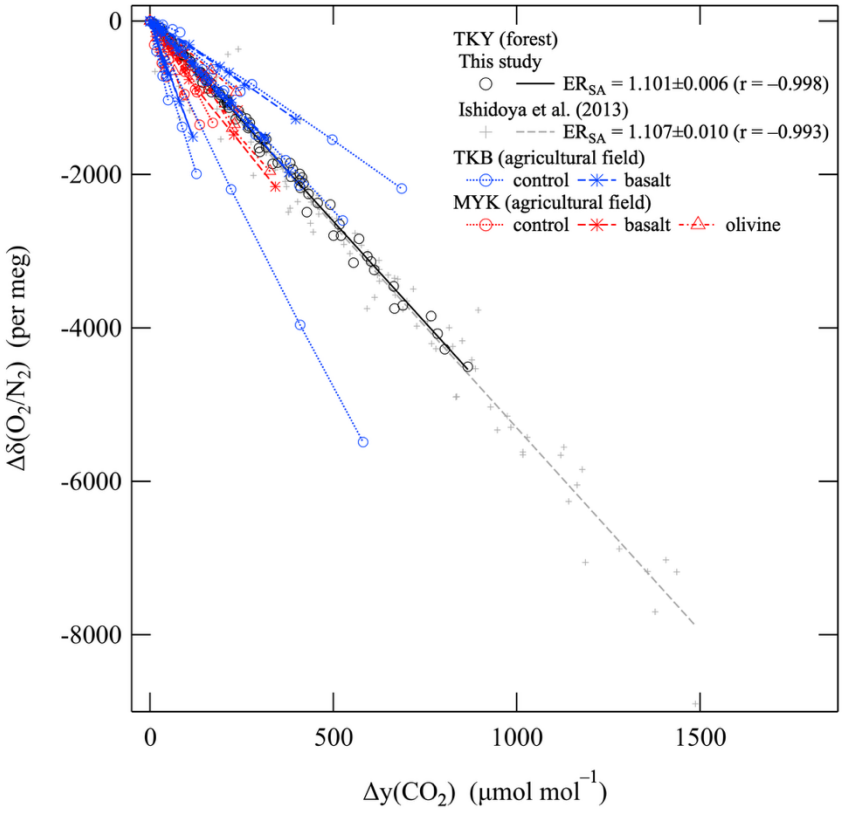

782

783 **Figure 6.** Relationships between $\Delta\delta(O_2/N_2)$ and $\Delta y(CO_2)$ at TKY, MYK, and TKB. $\Delta\delta(O_2/N_2)$ and $\Delta y(CO_2)$ were calculated from the data
784 shown in Figs. 2–4 by subtracting the measured value of the first sample from the subsequent samples for each soil chamber experiment.
785 The black solid line denotes the least-squares regression line fitted to the data at TKY. The corresponding relationships at TKY from August
786 2004 to October 2006, and from July 2011 to October 2012 reported by Ishidoya et al. (2013) are also shown.

787

788

789

790

791

https://doi.org/10.5194/egusphere-2026-2751
Preprint. Discussion started: 16 June 2026

792

793 (a)

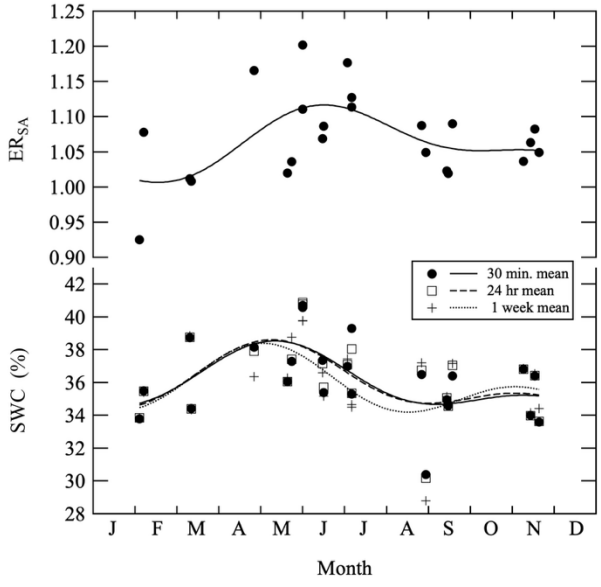

794

795 (b)

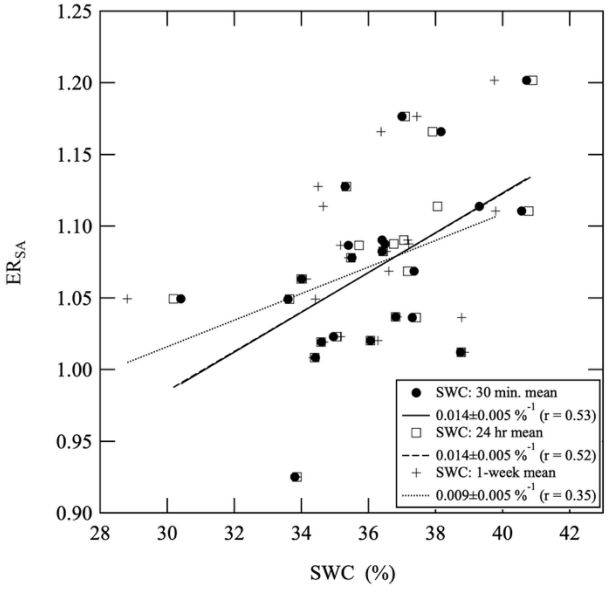

796

797 **Figure 7.** (a) Seasonal variations of ER_{SA} at TKY shown in Fig. 2a. The 30-min, 24-h, and 1-week mean values of soil water content (SWC)
798 at a depth of 15 cm observed at the same time as the soil chamber measurements are also shown. The average seasonal cycles modeled by a
799 fundamental sine–cosine and its first harmonic with respective periods of 12 and 6 months are also shown. (b) Relationship between ER_{SA}

https://doi.org/10.5194/egusphere-2026-2751
Preprint. Discussion started: 16 June 2026

and 30-min mean values of SWC in (a). The solid line denotes the least-squares regression line fitted to the data. The same relationships and regression lines for the 24-h and 1-week mean values of SWC are also shown.

https://doi.org/10.5194/egusphere-2026-2751
Preprint. Discussion started: 16 June 2026

803
804
805

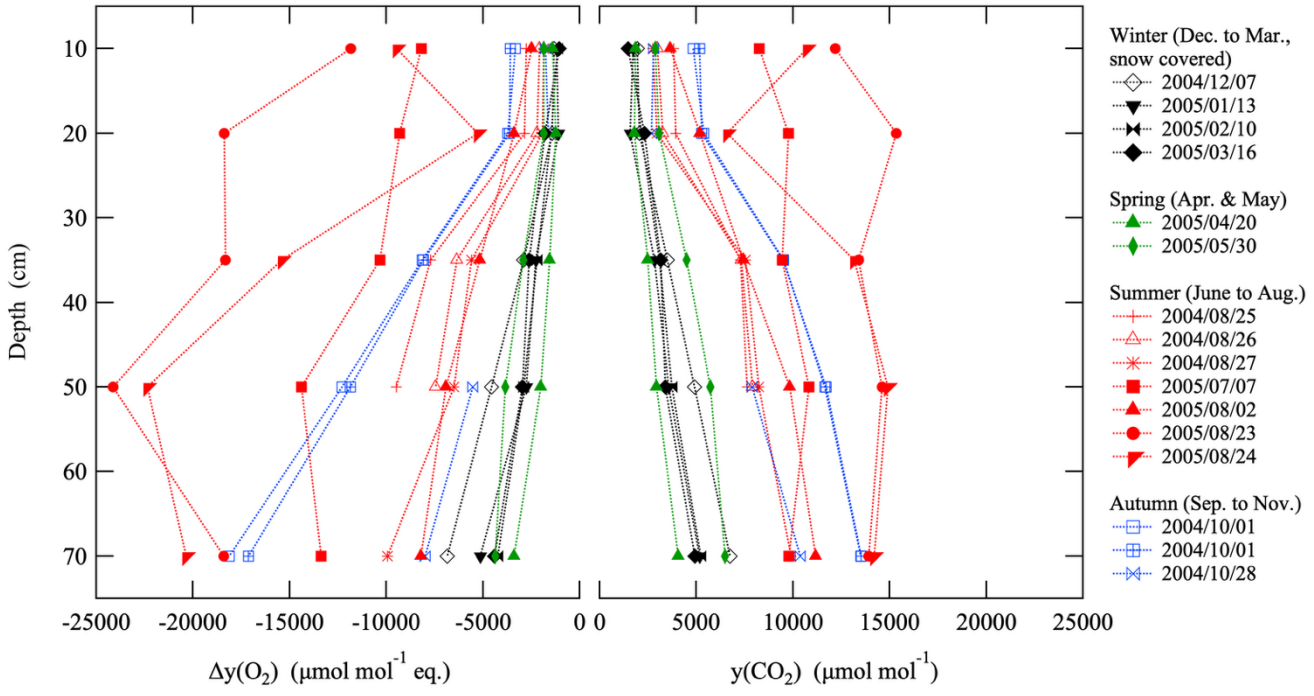

806
807

808 **Figure 8.** Vertical profiles of $\Delta y(O_2)$ and $y(CO_2)$ in soil pore air at TKY for the period 25 August 2004 to 24 August 2005. Δ denotes
809 deviations of $y(O_2)$ in soil pore air from the atmospheric value at TKY during 2004–2005.

810

https://doi.org/10.5194/egusphere-2026-2751
Preprint. Discussion started: 16 June 2026

811 (a)

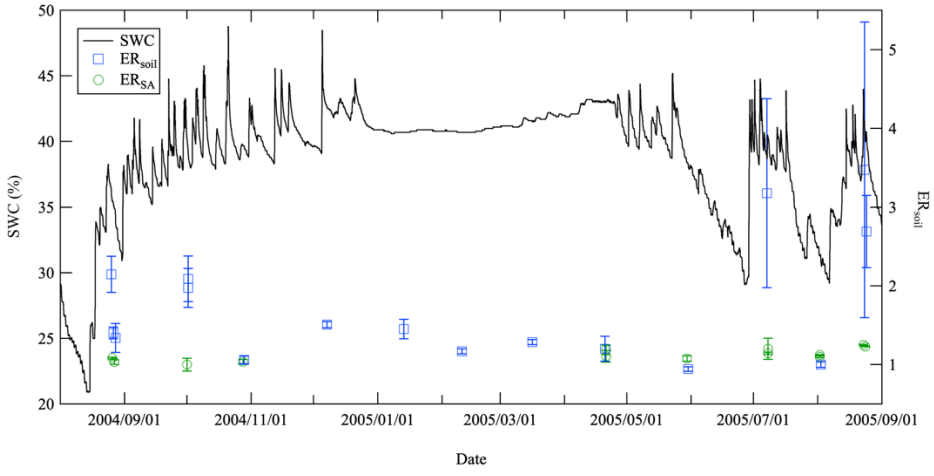

812

813 (b)

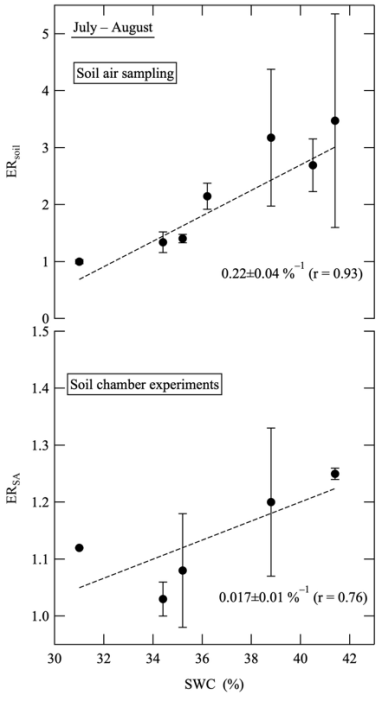

814

815

816 **Figure 9.** (a) 30-min mean values of SWC at a depth of 15 cm and ER_{soil} observed at TKY for the period 1 August 2004 to 31 August 2005.
817 The ER_{SA} values observed during the period are also shown, except for ER_{SA} during the snow-covered period. (b) Relationships of ER_{soil}
818 and ER_{SA} with SWC during July and August of 2004 or 2005. Black dashed lines denote the least-squares regression lines fitted to the data.

819

https://doi.org/10.5194/egusphere-2026-2751
Preprint. Discussion started: 16 June 2026

820 (a)

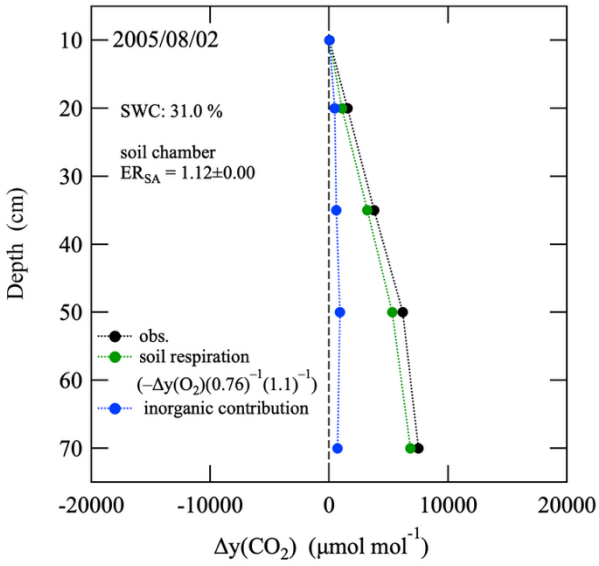

821

822 (b)

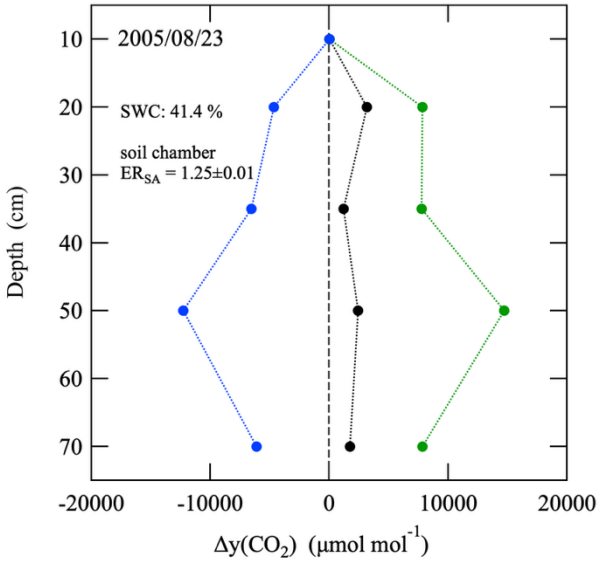

823

824 **Figure 10.** (a) Vertical profile of $\Delta y(CO_2)$ in soil pore air at TKY on 2 August 2005. Δ denotes deviations of $y(CO_2)$ at each depth from the
825 value at a depth of 10 cm. The contributions of soil respiration and inorganic processes to $\Delta y(CO_2)$, estimated from simultaneous analysis
826 of $\Delta y(O_2)$ and $\Delta y(CO_2)$ by assuming an OR of 1.1 for soil respiration, are also shown (see text for details). Thirty-minute mean values of
827 SWC when the vertical profiles of $\Delta y(CO_2)$ were observed, and values of ER_{SA} observed on the same day, are also indicated in the figure.
828 (b) Same as in (a) but for 23 August 2005.

https://doi.org/10.5194/egusphere-2026-2751
Preprint. Discussion started: 16 June 2026

829

830 (a)

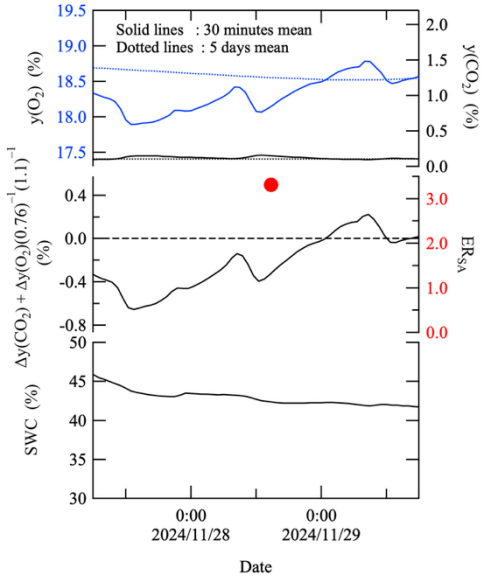

831

832 (b)

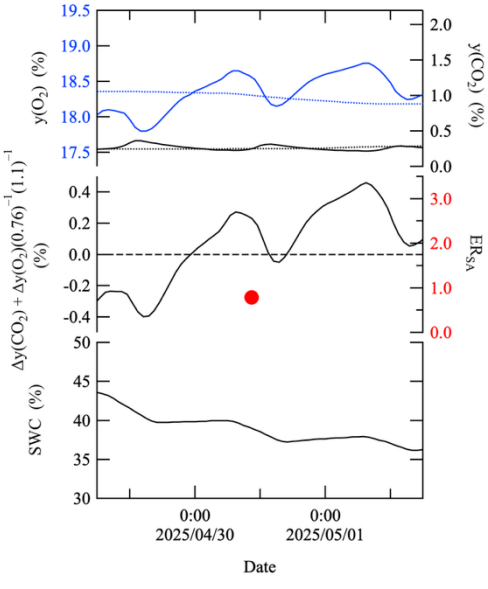

833

834 (c)

https://doi.org/10.5194/egusphere-2026-2751
Preprint. Discussion started: 16 June 2026

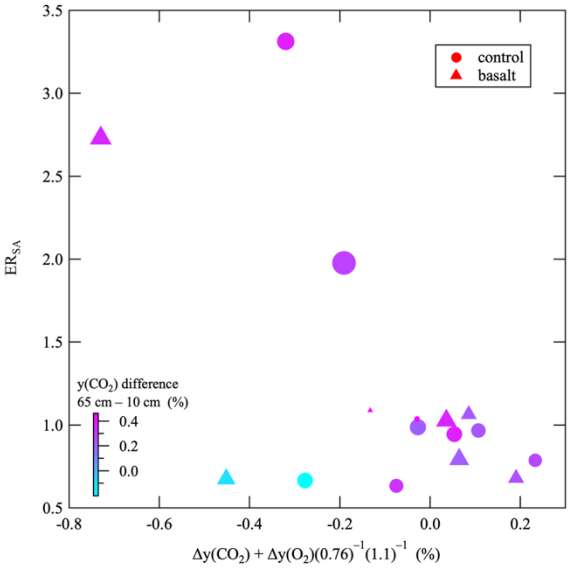

Figure 11. (a) (top panel) 30-min and 5-day mean values of $y(O_2)$ and $y(CO_2)$ in soil pore air at a depth of 10 cm observed at TKB from 06:00 (JST) on 27 November to 18:00 on 29 November 2024. (middle panel) $\Delta y(CO_2) + \Delta y(O_2)(0.76)^{-1}(1.1)^{-1}$, which represents the contribution of inorganic processes (see text for details), and the observed ER_{SA} at the plots with planting, with chemical fertilizer, and without spreading of crushed basalt at TKB are also shown (see Fig. 4a). Δ denotes the differences of $y(O_2)$ or $y(CO_2)$ calculated by subtracting their 5-day mean values from the 30-min mean values. (bottom panel) SWC values at a depth of 10 cm. (b) Same as in (a) but from 06:00 on 29 April to 18:00 on 1 May 2025. (c) Relationship between ER_{SA} and $\Delta y(CO_2) + \Delta y(O_2)(0.76)^{-1}(1.1)^{-1}$ in the plots with planting, with chemical fertilizer, and with or without application of crushed basalt at TKB for the period November 2024 to October 2025. Marker size increases with increasing SWC. Differences of $y(CO_2)$ calculated by subtracting the $y(CO_2)$ at a depth of 10 cm from those at a depth of 65 cm are shown by the color scale.

https://doi.org/10.5194/egusphere-2026-2751
Preprint. Discussion started: 16 June 2026

851 (a)

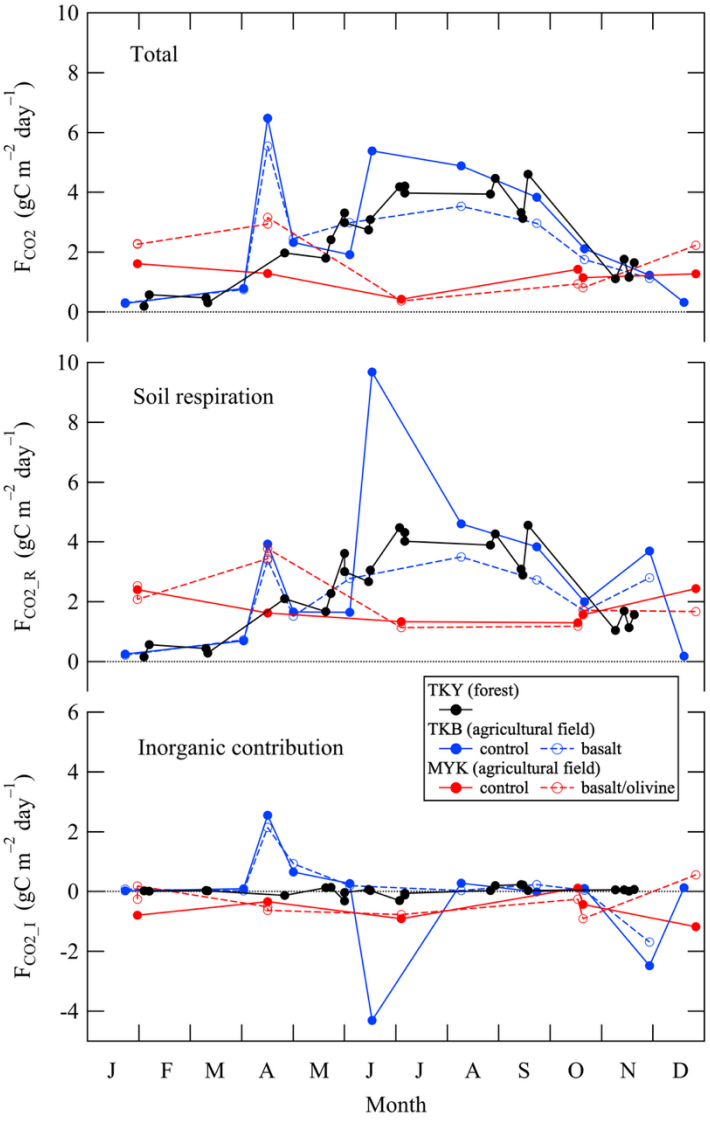

852
853
854

https://doi.org/10.5194/egusphere-2026-2751
Preprint. Discussion started: 16 June 2026

855 (b)

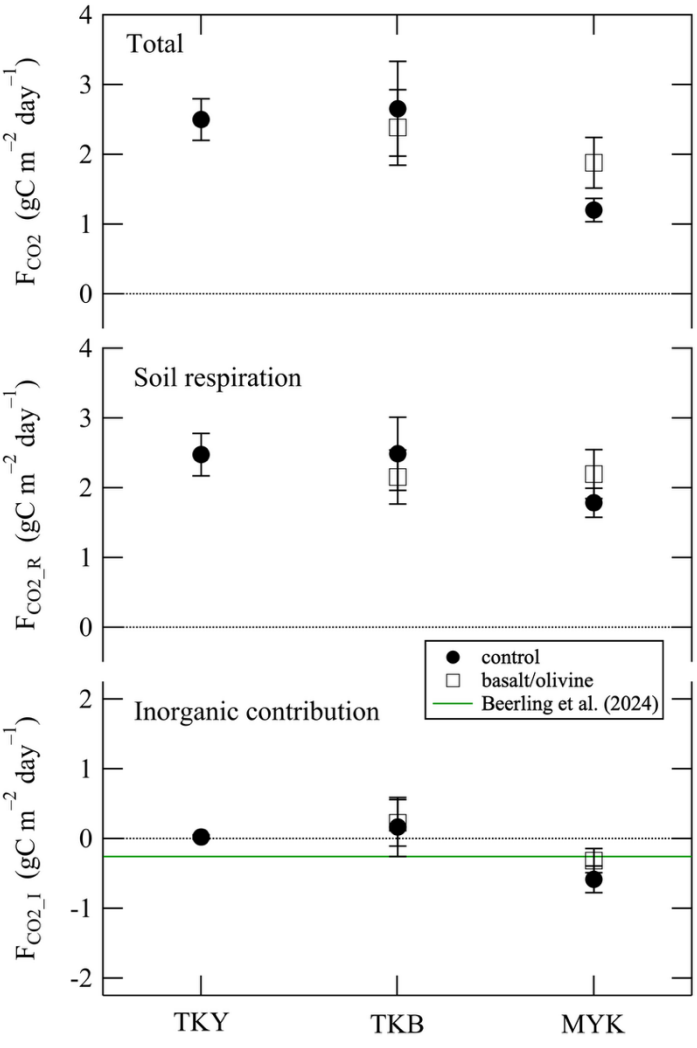

856
857
858 **Figure 12.** (a) (top panel) Seasonal variations of soil–air CO_2 flux (F_{CO2}) observed by soil chamber experiments at TKY, TKB, and MYK.
859 (middle panel) Contributions of soil respiration (F_{CO2_R}) to F_{CO2}, and (bottom panel) contributions of inorganic processes (F_{CO2_I}) to F_{CO2}
860 are also shown. The labels "control" and "basalt" for TKB represent the planted plots fertilized by chemical fertilizer without and with
861 crushed basalt, respectively, which correspond to the data indicated by black and red markers in Fig. 4. For MYK, "control" and
862 "basalt/olivine" are the same definitions given in the caption of Fig. 5. Positive values denote CO_2 emission from the soil to the atmosphere.
863 (b) Average F_{CO2} throughout the observation periods, and average values of F_{CO2_R} and F_{CO2_I}. The data at TKB were calculated by averaging
864 for the period when both "control" and "basalt" data were available. Error bars indicate ±1 standard error based on the number of observations

https://doi.org/10.5194/egusphere-2026-2751
Preprint. Discussion started: 16 June 2026

($\boldsymbol{\sigma/\sqrt{n}}$). The green line denotes F_{CO2_I} calculated from the carbon dioxide removal (CDR) rate of 3.4 t CO_2 ha^{-1} $year^{-1}$ for enhanced rock weathering (ERW) reported by Beerling et al. (2024).

https://doi.org/10.5194/egusphere-2026-2751
Preprint. Discussion started: 16 June 2026

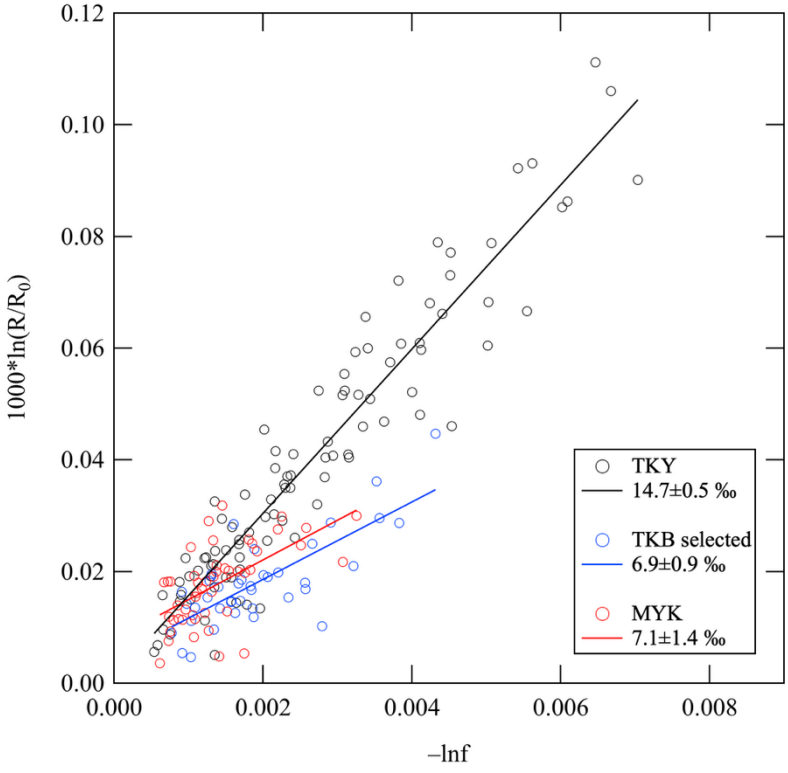

Figure 13. Relative changes in the isotopic composition of O_2 as a function of the natural logarithm of the remaining O_2 fraction (see Eq. 12 in text) at TKY, TKB, and MYK. The slopes of the least-squares regression lines fitted to the data give the isotopic discrimination for soil respiration, ε_{SR}. The plotted data are calculated from $\delta_{atm}(^{18}O)$ and $\delta(O_2/N_2)$ in Figs. 3b, 4b, and 5b, but those with r^2 values lower than 0.5 (indicated by gray text in the figure legends) are excluded. At TKB, the data observed on 28 November 2024 as well as 15 April and 16 July 2025, which showed substantial F_{CO2_I} in Fig. 12a, are also excluded.

https://doi.org/10.5194/egusphere-2026-2751
Preprint. Discussion started: 16 June 2026

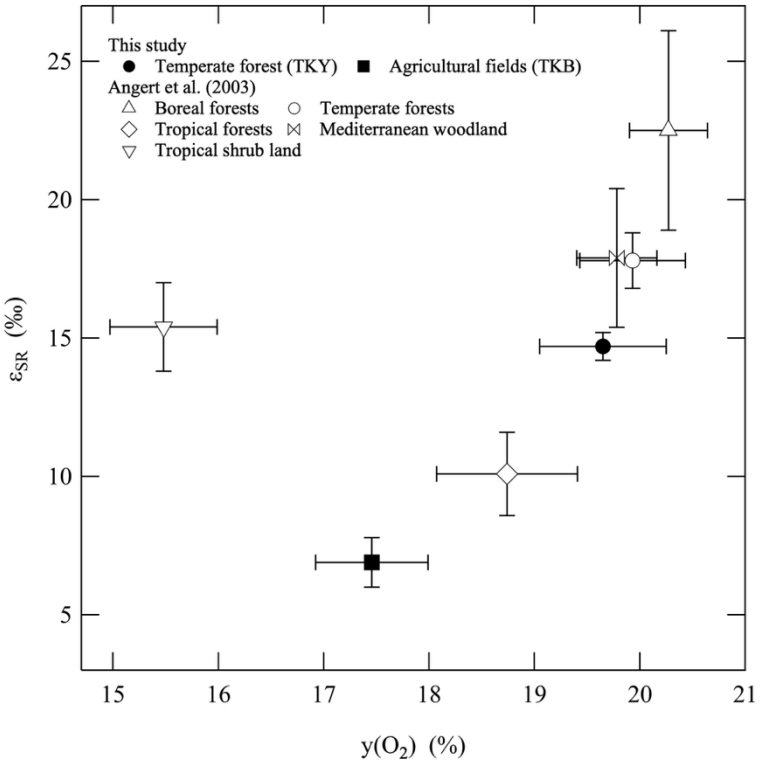

878

879 **Figure 14.** Values of ε_{SR} at TKB shown in Fig. 13 plotted against $y(O_2)$ at a depth of 65 cm in soil pore air. The ε_{SR} values at TKY plotted
880 against average $y(O_2)$ at depths of 50 and 70 cm in soil pore air are also shown. The ε_{SR} values plotted against $y(O_2)$ at depths of 40–155 cm
881 in soil pore air in boreal forests, temperate forests, tropical forests, Mediterranean woodland, and tropical shrub land reported by Angert et
882 al. (2003) are also shown.

883